Light adaptation in turtle cones

Testing and analysis of a model for phototransduction

Daniel Tranchina, James Sneyd, and Isabel D. Cadenas

Department of Biology, Courant Institute of Mathematical Sciences, and Center for Neural Science, New York University, New York, New York 10003; Department of Biomathematics, University of California at Los Angeles School of Medicine, Los Angeles, California 90024; and Department of Biology, New York University, New York, New York 10003 USA

ABSTRACT Light adaptation in cones was characterized by measuring the changes in temporal frequency responses to sinusoidal modulation of light around various mean levels spanning a range of four log units. We have shown previously that some aspects of cone adaptation behavior can be accounted for by a biochemical kinetic model for phototransduction in which adaptation is mediated largely by a sigmoidal dependence of guanylate cyclase activity on the concentration of free cytoplasmic Ca^{2+}, ($[Ca^{2+}]_i$)(Sneyd and Tranchina, 1989). Here we extend the model by incorporating electrogenic Na^+/K^+ exchange, and the model is put to further tests by simulating experiments in the literature. It accounts for (*a*) speeding up of the impulse response, transition from monophasic to biphasic waveform, and improvement in contrast sensitivity with increasing background light level, I_0; (*b*) linearity of the response to moderate modulations around I_0; (*c*) shift of the intensity-response function (linear vs. log coordinates) with change in I_0 (Normann and Perlman, 1979); the dark-adapted curve adheres closely to the Naka-Rushton equation; (*d*) steepening of the sensitivity vs. I_0 function with $[Ca^{2+}]_i$ fixed at its dark level, $[Ca^{2+}]_i^{dark}$; (Matthews et al., 1988, 1990); (*e*) steepening of the steady-state intensity-response function when $[Ca^{2+}]_i$ is held fixed at its dark level (Matthews et al., 1988; 1990); (*f*) shifting of a steep template saturation curve for normalized photocurrent vs. light-step intensity when the response is measured at fixed times and $[Ca^{2+}]_i$ is held fixed at $[Ca^{2+}]_i^{dark}$ (Nakatani and Yau, 1988). Furthermore, the predicted dependence of guanylate cyclase activity on $[Ca^{2+}]_i$ closely matches a cooperative inhibition equation suggested by the experimental results of Koch and Stryer (1988) on cyclase activity in bovine rods. Finally, the model predicts that some changes in response kinetics with background light will still be present, even when $[Ca^{2+}]_i$ is held fixed at $[Ca^2]_i^{dark}$.

INTRODUCTION

In the process of light adaptation, sensitivity and dynamics of the responses of visual neurons adjust to the level of ambient illumination. It appears that one function of light adaptation is to present to the brain a retinal output which depends as closely as possible on the contrast in visual scenes rather than on absolute light levels. This is an effective strategy for dealing with the fact that while the physiological range of light levels from starlight to broad daylight is roughly 10 log units, the effective dynamic range of neural responses is only about two log units (Shapley and Enroth-Cugell, 1984).

Evidence indicates that light adaptation in turtle cones arises as a consequence of mechanisms internal to the cone. In particular, it appears that light adaptation in turtle cones is a direct result of the biochemical and electrophysiological processes underlying phototransduction; neural feedback from horizontal cells to cones in the turtle retina (Baylor et al., 1971; O'Bryan, 1973; Burkhardt et al., 1988) does not seem to play an important part in adaptation in cones or horizontal cells (Baylor and Hodgkin, 1974; Normann and Perlman, 1979; Naka et al., 1987; Itzhaki and Perlman, 1987). Moreover, a recent study by Matthews et al. (1990) has shown that all the hallmarks of light adaptation, evident in the voltage responses of cones and horizontal cells, are also present in the light-sensitive current in the outer segments of tiger salamander cones.

In recent years rapid advances have been made in understanding the molecular mechanisms underlying phototransduction (for reviews cf. Lamb, 1986; Baylor 1987; Pugh and Cobbs, 1986; Stryer, 1986; Stieve, 1986; Liebman et al., 1987; Yau and Baylor, 1989; Fain and Matthews, 1990; Pugh and Lamb, 1990). Recent work has linked calcium to light adaptation via control of guanylate cyclase activity (Koch and Stryer, 1988; Matthews et al. 1988; Nakatani and Yau, 1988). However, despite the enormous progress in unraveling the biochemical mechanisms of phototransduction, it has not yet been shown that our current understanding of these processes accounts fully for the electrophysiological behavior of photoreceptors in various states of adaptation. Progress along these lines has been reported by Forti et al. (1989), Sneyd and Tranchina (1989), and Nakatani et al. (1990).

In a previous paper (Sneyd and Tranchina, 1989) we used frequency-domain analysis as a tool to develop a

Address correspondence to Daniel Tranchina, Dept. of Biology, New York University, 1009 Main Building, 100 Washington Square East, New York, NY 10003.

0006-3495/91/07/217/21 $2.00

mathematical model for phototransduction. The Sneyd and Tranchina model for transduction in cones is similar to a model for transduction in rods presented by Forti et al. (1989). This model, which incorporates recently acquired information on underlying molecular mechanisms, accounts quantitatively for first-order frequency responses (linear-regime behavior) of turtle cones over a broad range of light levels. The approach to modeling phototransduction by measuring and fitting adaptation behavior has been taken before in the pioneering work of Baylor et al. (1974*a*, *b*). However, their model, based on the blocking-particle hypothesis, was developed long before the identity of the internal transmitter and the steps linking its concentration to light had been firmly established.

The emphasis of this largely theoretical paper is on (*a*) the physiological underpinnings and implications of our previous model for phototransduction (Sneyd and Tranchina, 1989) which we extend here to include electrogenic Na^+/K^+ exchange, and (*b*) testing of the model, by comparison with experimental results in the literature, under conditions of fixed and normal intracellular Ca^{2+} concentration.

For a detailed treatment of technical and mathematical aspects of the model, including the derivation of the equations, the mathematical justification of simplifications, and the curve fitting techniques, the reader is referred to Sneyd and Tranchina (1989).

MODEL

A diagram of the kinetic scheme in the model for phototransduction described below is given in Fig. 1. The following is a detailed discussion of the physiological basis and implications of the assumptions used in the derivation of the equations in a complementary mathematical paper (Sneyd and Tranchina, 1989). Similar arguments and equations have been used by Hodgkin and Nunn (1988) and by Forti et al. (1989) in modeling various aspects of rod transduction.

(*a*) The number of open light-sensitive channels in the cone outer segment membrane is determined by the free cyclic GMP (cGMP) concentration, $[cGMP]^{free}$, in a cooperative manner. Haynes and Yau (1985) found a Hill coefficient n in the range of 1.6–3. Our computations indicate that linear-regime behavior of the model is fairly insensitive to n; that is, several different values of n give equally good fits of the model to linear-regime data. However, the steepness of the intensity-response function is more realistic with higher values of n. All computations in this paper were done with $n = 3$.

(*b*) The dependence of the total light-sensitive current on voltage in turtle cones follows the approximately exponential relationship, found by Haynes and Yau (1985) for single cGMP-gated channels in catfish cone outer segments, over the physiological range of membrane potentials.

(*c*) A small fraction of the inward light-sensitive current is carried by Ca^{2+} (Yau and Nakatani, 1985). In the earlier model (Sneyd and Tranchina, 1989), we assumed this fraction is independent of membrane potential. This assumption simplifies computations in the model; it also allows one to compute an analytic

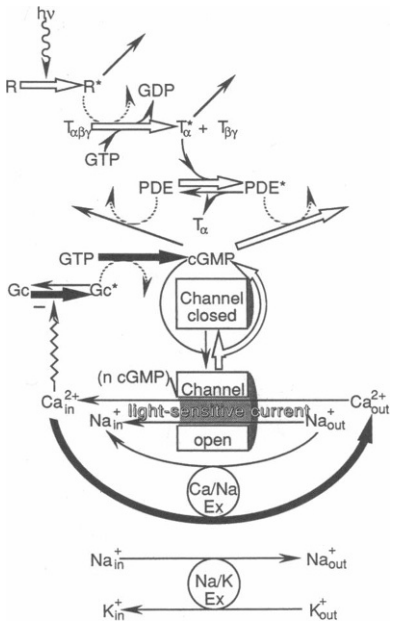

FIGURE 1 A reaction scheme for phototransduction. Open arrows denote reactions in the feed-forward pathway (i.e., the excitation pathway that leads to the breakdown of cGMP and closure of the light-sensitive channels), and filled arrows denote reactions in the feedback pathway (i.e., the reactions, leading to the restoration of cGMP, that cause light adaptation). Dashed lines indicate catalysis. The effect of $[Ca^{2+}]_i$ on the activity of guanylate cyclase is denoted by a saw-toothed arrow with a minus sign. This set of reactions is not modeled in detail but is instead modeled by an instantaneous nonlinear function (see text for details): the minus sign indicates that Ca^{2+} has an inhibitory effect on the activity of guanylate cyclase. The terms are defined as follows: R^*, activated cone pigment; T_α^*, activated transducin; PDE*, activated phosphodiesterase; Gc*, activated guanylate cyclase; Ca/K Ex, Na^+/Ca^{2+}-K^+ exchange pump; Na/K Ex, Na^+/K^+ exchange pump. Note that (*a*) in the dark there is continual turnover of cGMP and a continual influx of Ca^{2+} through the light-sensitive channels; (*b*) the effect of light is to increase the hydrolysis of cGMP (due to the increased concentration of PDE*), and thus to close the light-sensitive channels; (*c*) as a result of closure of the light-sensitive channels the internal levels of Ca^{2+} falls, which in turn increases the activity of guanylate cyclase; (*d*) this increase in the rate of production of cGMP is a form of negative feedback.

expression for the dependence of guanylate cyclase activity on $[Ca^{2+}]$. This assumption is unlikely to be correct because Ca^{2+} is divalent, whereas Na^+ is monovalent. Nevertheless, no obvious improvement in our model's behavior is obtained by choosing a steeper *i/v* relationship for the light-sensitive current carried by Ca^{2+}. Therefore, for all the present computations, we retain our original simplifying assumption.

(*d*) The outward K^+ current in the inner segment is carried through ohmic channels of fixed conductance. Attwell et al. (1982) found that a voltage-sensitive conductance in tiger salamander cones made only a small contribution to shaping their voltage responses to light. However, Maricq and Korenbrot (1990) have recently reported on an inward-rectifying K^+ current in lizard cones which is likely to make a substantial contribution in shaping their light-evoked responses. There is some indirect evidence that a similar conductance may play an important role in turtle cones (see Discussion).

(*e*) A Na^+/Ca^{2+}-K^+ exchange pump in the outer segment (Yau and Nakatani, 1984) pumps out Ca^{2+} at a rate proportional to the free cytoplasmic Ca^{2+} concentration ($[Ca^{2+}]_i$). This assumption is consistent with the observation of an exponential decay of pump current in rods following the onset of bright, steady illumination which shuts off the light-sensitive current (Hodgkin et al., 1987; Yau and Nakatani, 1985); similar but faster currents have been observed in cones (Yau and Nakatani, 1988; Cobbs and Pugh, 1986). Light causes a reduction in $[Ca^{2+}]_i$ (Ratto et al., 1988) because closure of the light-sensitive channels restricts the entry of Ca^{2+} while it continues to be pumped out by the Na^+/Ca^{2+}-K^+ exchange pump (Yau and Nakatani, 1985). The stoichiometry for this exchanger of 4 Na^+ in for 1 K^+ and 1 Ca^{2+} out (Cervetto et al., 1989) is used in the model equations below. We ignore the dependence of the pump rate on membrane potential (Langando et al., 1988; Cervetto et al., 1989).

(*f*) In dark-adapted rods, and presumably cones as well, there is a constant turnover of cGMP (Goldberg et al., 1983; Dawis et al., 1988). In the model, we account for this turnover by assuming that the dark (inactivated) form of cGMP-phosphodiesterase (PDE) has some catalytic activity, but less than that of the light-activated form (PDE*). An alternative mechanism not considered here, which would also give a turnover of cGMP in the dark, is spontaneous, light-independent activation of the inactivated form of PDE that has *no* catalytic activity. This would occur if the catalytic and inhibitory subunits of PDE are not tightly bound, but rather the complex is in equilibrium with the dissociated subunits. This alternative, although more complicated to model, may be more consistent with the pronounced voltage noise of cones in darkness (cf. Lamb, 1987, for review). However, we believe that these alternative models cannot be distinguished by our experiments for the following reason. Although the two alternatives lead to somewhat different saturation curves for PDE* vs. background light, computations with the model indicate that PDE is far from saturation for every one of our experimental light levels but the highest. Thus, our experiments barely extend into the region in which these alternative models are distinguishable, and certainly do not provide sufficient information to enable us to say with certainty which is the more accurate model.

In the model, the α-subunit of transducin (G-protein) with GTP bound, T_α-GTP (T_α^*), converts PDE to PDE* in a bimolecular reaction. Because PDE* has greater catalytic activity than PDE, light causes the rate of hydrolysis of cGMP to increase and $[cGMP]^{free}$ to decrease. Furthermore, the K_m for each form of the enzyme is assumed to be large compared with $[cGMP]^{free}$ (Sitaramayya et al., 1986; Barkdoll et al., 1986), and large compared with the concentration of the corresponding enzyme. These assumptions imply firstly that the rate of cGMP hydrolysis by each form of the enzyme is approximately proportional to the product of enzyme and substrate concentrations, and secondly, that the phosphodiesterase bound up in the enzyme-substrate complex can be ignored in the conservation (rate) equation for phosphodiesterase (Sneyd and Tranchina, 1989).

(*g*) Cyclic GMP is synthesized, from an abundant concentration of GTP, by guanylate cyclase at a rate which depends on $[Ca^{2+}]_i$ (Lolley and Racz, 1982; Koch and Stryer, 1988; Hodgkin and Nunn, 1988; Detwiler and Rispoli 1989; Kawamura and Murakami; 1989). We assume that modulation of guanylate cyclase activity by Ca^{2+} occurs on a fast time scale, so that the rate of cGMP synthesis is modeled as an instantaneous function of $[Ca^{2+}]_i$. To be more precise, we are assuming that Ca^{2+} controls guanylate cyclase activity on a time scale which is fast compared with the time scale of change in $[Ca^{2+}]_i$. The functional form of this dependence is derived by constraining the steady-state input-output relation of the model to follow that measured experimentally (Sneyd and Tranchina, 1989). We will show that the dependence of cyclase activity on $[Ca^{2+}]$ predicted in this way matches closely an analytical expression based on the experimental measurements of Koch and Stryer (1988), who demonstrated cooperative inhibition of guanylate cyclase activity by Ca^{2+} in bovine rods. The only site of Ca^{2+} feedback in the model is on guanylate cyclase; this is consistent with the recent results of Barkdoll et al. (1989) which argue against Ca^{2+} regulation of any steps involved in the activation or deactivation of phosphodi-

esterase, for physiological levels of $[Ca^{2+}]_i$. A model parameter which has little effect on the linear-regime behavior of the model is δ, the rate of cGMP synthesis in the dark; it is chosen arbitrarily so that the free cGMP concentration turns over 5 times/s in darkness. This assumed rate is considerably higher than that estimated for salamander rods by Hodgkin and Nunn (1988). The higher value is not *required* in the model, but it appears from our computations that much lower values do require a larger dynamic range for guanylate cyclase activity.

(*h*) The steps by which T_α-GTP (activated transducin) is produced are approximated as a multistage linear process. For the sake of simplicity, we assume that T_α-GTP is produced by a process which is phenomenologically equivalent to a cascade of four first-order reactions (Baylor et al., 1974*b*) with identical time constants. Four stages are necessary to obtain sufficient response delay, which is reflected in phase lag in the temporal frequency response. The data and analysis of Wessling-Resnick and Johnson (1987) suggest that activation of transducin proceeds by a double-displacement catalytic mechanism. This mechanism provides plenty of room for four stages or more between absorption of a photon and production of activated transducin.

We assume also that the conversion of PDE to PDE* does not use up a significant fraction of T_α-GTP. The implicit assumption is that most of the T_α-GTP molecules decay before encountering PDE. Furthermore, PDE* decays at a rate proportional to its concentration, as the GTP-ase activity of T_α catalyzes the T_α-GTP to T_α-GDP conversion. First-order kinetics for the decay of PDE* is indicated by the experimental results of Kawamura and Murakami (1986) and Hodgkin and Nunn (1988). We assume that the PDE-T_α-GTP complex dissociates "immediately" to PDE and T_α-GDP upon the hydrolysis of GTP. The assumptions above imply that [T_α-GTP] depends linearly on the light stimulus. Although this is surely not the case for very high light levels, we hypothesize that nonlinearities in the transducin kinetics play no essential role in light adaptation over a broad range of low to fairly high light levels. Therefore, we believe it is a good idea to simplify the first stages of transduction and to focus attention on the calcium feedback mechanism of adaptation.

(*i*) The contribution of the Na^+/Ca^{2+}-K^+ exchange pump in the outer segment to the total membrane current is small compared with the light-sensitive current (Pugh and Cobbs, 1986).

(*j*) The rate of the electrogenic Na^+/K^+ exchange pump is proportional to $[Na^+]_i$ (Torre, 1982), and the ratio of Na^+ out to K^+ in is 3:2.

(*k*) The cone contains a number of cGMP binding sites with high affinity, so that $[cGMP]^{free}$ is a small fraction of $[cGMP]^{total}$ (Pugh and Cobbs, 1986). Moreover, the high-affinity binding sites do not release their cGMP until $[cGMP]^{free}$ drops to a very low level. Thus, large relative changes in $[cGMP]^{free}$ can occur with relatively little change in $[cGMP]^{total}$ (Sneyd and Tranchina, 1989). Therefore, the tightly bound pool of cGMP plays no role in our model. Hereafter, we will simply use [cGMP] to denote $[cGMP]^{free}$.

(*l*) The cone contains a large-capacity, low-affinity Ca^{2+}-buffer system. Rapid equilibration between free and bound pools of Ca^{2+} make the free concentration of Ca^{2+} a small fraction of the total at every instant. Consequently, only a small fraction of i_{Ca} through the light-sensitive channels contributes to changes in free cytoplasmic Ca^{2+}. As shown by Sneyd and Tranchina (1989), the assumption of a Ca^{2+} buffer is necessary to obtain consistency between the best-fit model parameters and the estimated size of the Ca^{2+} component of the light-sensitive current. Although Ca^{2+} interacts with guanylate cyclase, the amount of Ca^{2+} involved in this interaction is ignored in the conservation equation for Ca^{2+} on the assumption that it is a small fraction of the total intracellular Ca^{2+}.

(*m*) Over a broad range of light levels, the steady-state polarization $V_0 = v_0 - v_{dark}$ is related to the steady illumination I_0 by

$$V_0 \approx -k_1 \ln (1 + k_2 I_0). \tag{1}$$

Eq. 1 fits well the steady-state data in Figs. 1 and 7 of Normann and Perlman (1979) and our own steady-state data (two cells) in this study. The validity of Eq. 1 is also supported by combining the findings of several previous studies: (*a*) Itzhaki and Perlman (1987) found that sensitivity and steady polarization of turtle cones are related by the equation

$$-\log (S_F/S_F^D) \approx 4.7 (V_0/V_{max}), \tag{2}$$

where S_F is the cone sensitivity with a steady illumination I_0 which gives a steady polarization V_0; S_F^D is the dark-adapted sensitivity; V_{max} is the maximal cone polarization. (*b*) Copenhagen and Green (1987) and Baylor and Hodgkin (1974) found that the sensitivity of turtle cones is related to I_0 by the equation

$$S_F/S_F^D = (1 + I_0/I_*)^{-1}, \tag{3}$$

where I_* is the steady light level that reduces the sensitivity by a factor of 2. Putting together Eqs. 2 and 3 gives

$$V_0 = 0.21 V_{max} \log (1 + I_0/I_*), \tag{4}$$

or

$$V_0 = 0.092 V_{max} \ln (1 + I_0/I_*). \tag{5}$$

Note that Eq. 5 is of the same form as Eq. 1 (i.e., with $k_1 = 0.092V_{max}$ and $k_2 = I_*^{-1}$).

One implication of Eq. 1 is that, over a broad range of light levels, the steady membrane polarization is linearly related to the logarithm of the steady illumination. For high enough light levels, $k_2I_0 \gg 1$, so that $V_0 \approx -k_1 \ln(k_2I_0) = -2.3 \log I_0 - 2.3k_1 \log k_2$. Thus, over the range of light levels where this approximation holds, every log unit of light leads to a hyperpolarization of $-2.3k_1$ (mV). Our experimental measurements on two cones indicate a 3–4 mV hyperpolarization per log unit of light. The cone illustrated by Normann and Perlman (1979, Fig. 6) shows a 7.2-mV hyperpolarization for a 2.15 log-unit increment of steady light, i.e., 3.5 mV per log unit. In addition, their finding that the ratio of the final steady polarization to the initial peak polarization was ~0.4, for each steady background illumination (Normann and Perlman, 1979, Fig. 1) can be shown to be consistent with a hyperpolarization of ~4 mV per log unit of light, for a typical cell with a 20-mV maximal hyperpolarization. That is, it can be shown that, given the Naka–Rushton relation, $V_{peak} = V_{max}I_0/[\sigma + I_0]$, and the fact that $V_0 = 2.3k_1 \log[1 + k_2I_0]$ (Eq. 1), the constraint that $V_0/V_{peak} \sim 0.4$ requires that $2.3k_1 \sim 0.2V_{max}$. Then, every log unit of steady light will give a hyperpolarization of $0.2V_{max}$.

Still further evidence for the validity of Eq. 1 comes from the results of Matthews et al. (1988) which show an approximately logarithmic dependence of steady photocurrent on steady light, over a broad range of light levels and under conditions of physiological $[Ca^{2+}]_i$.

Summary of equations of previous model ignoring Na^+/K^+ exchange

As shown by Sneyd and Tranchina (1989), when electrogenic Na^+/K^+ exchange is ignored, the above assumptions, together with approximations which are valid in the physiological regime of concentrations and voltages, lead to a simple set of differential equations. We restate the equations of the original model below in simplified notation, and then show how the equations are modified when Na^+/K^+ exchange is included. The definitions of the dynamic variables and interpretations of the model constants in the following kinetic equations are given in Table 1 and Table 2, respectively.

$$\frac{dp}{dt} = s(t)(1 - p) - \beta p \tag{6}$$

$$\frac{dx}{dt} = g(y) - \delta x - \gamma p x \tag{7}$$

TABLE 1 **Physiological interpretation of dynamic variables**

p	Fraction of PDE which is in the activated form (i.e., $p = [PDE^*]/[PDE]^{tot}$).
x	Concentration of cGMP measured as a fraction of the dark level (i.e., $x = [cGMP]/[cGMP]_{dark}$).
g	Rate of synthesis of cGMP measured in units of $[cGMP]_{dark}$; i.e., $g = 5\,s^{-1}$ means a synthesis rate of 5 $[cGMP]_{dark}\,s^{-1}$.
y	Concentration of Ca^{2+} measured as a fraction of the dark level (i.e., $y = [Ca^{2+}]_i/[Ca^{2+}]_i^{dark}$).
z	Concentration of Na^+ measured as a fraction of the dark level (i.e., $z = [Na^+]_i/[Na^+]_i^{dark}$).
V	Cone membrane potential measured relative to the value in darkness (i.e., $V = v - v_{dark}$) (dimension: millivolts).

$$\frac{dy}{dt} = \alpha(x^n e^{-V/v^*} - y) \tag{8}$$

$$\tau_m \frac{dV}{dt} = -Ex^n e^{-V/v^*} - (V - E), \tag{9}$$

where

$$s(t) = K_1[T_\alpha - GTP] = \int_{-\infty}^{t} I(t')\,h(t - t')\,dt', \tag{10}$$

I is light intensity in relative units (see Methods), and

$$h(t) = \frac{\eta}{3!\tau_1}\left(\frac{t}{\tau_1}\right)^3 e^{-t/\tau_1}, \quad \text{for} \quad t > 0. \tag{11}$$

The steady-state voltage of this system as a function of the background light level, I_0, is constrained to be of the form (Sneyd and Tranchina, 1989)

$$V_0 = -k_1 \ln\left(\frac{1 + k_2I_0}{1 + k_3I_0}\right), \tag{12}$$

where k_1 and k_2 are constants determined from the data and $k_3 = k_2 \exp(E/k_1)$. This is a simple extension of Eq. 1 which gives the required feature of saturation of steady polarization at high light levels. With this constraint (Eq. 12), the feedback function, $g(y)$, and the steady-state relations $[p_0(I_0)$, $x_0(I_0)$, and $y_0(I_0)]$ can be computed analytically by solving Eqs. 6–11 in the steady state.

Modifications to include electrogenic Na^+/K^+ exchange

Torre (1982) found that an electrogenic Na^+/K^+ exchange pump makes an important contribution to the electrical activity of toad rods. If a similar Na^+/K^+ exchange pump in the cone inner segment is electrogenic with a 3:2 ratio for Na^+_{out}/K^+_{in}, then it must make a

TABLE 2 **Physiological interpretation of constants**

τ_m	RC time constant of an isolated cone when all the light-sensitive channels are closed (dimensions: seconds).
α	Rate of decay of Na^+/Ca^{2+}-K^+ exchange-pump current and $[Ca^{2+}]_i$ when all light-sensitive channels are closed (dimensions: seconds^{-1}). The time constant for decay $\tau_\alpha = 1/\alpha$.
δ	Rate of cGMP hydrolysis in the dark measured in units of $[cGMP]_{dark}$; i.e., $\delta = 5\ s^{-1}$ means that the dark turnover rate of cGMP is 5 $[cGMP]_{dark}\ s^{-1}$. The rate of hydrolysis of cGMP by PDE per mole of cGMP and per mole of PDE is given by $\delta/[PDE]^{total}$ (dimension: seconds^{-1}).
γ	A combination of parameters which determines the hydrolytic rate of activated PDE (PDE*). The ratio of the hydrolyic rate of PDE* to that of PDE (specific activities) is given by $(\gamma + \delta)/\delta$. The hydrolytic rate of PDE* (corresponding to that of PDE above) is given by $(\gamma + \delta)/[PDE]^{total}$ (dimension: seconds^{-1}).
β	Rate constant for decay of PDE* back to PDE (dimensions: seconds^{-1}).
η	Determines the rate of activation of PDE. At a steady relative light level $I_0 = \beta/\eta$, half the PDE is in activated form (dimension: seconds^{-1}).
τ_1	The time constant for each of the initial four stages leading to the production of activated transducin (dimensions: seconds).
ν	Rate constant for the electrogenic Na^+/K^+ exchange pump. The time constant $\tau_\nu = 1/\nu$ was set equal to 25 s for all computations in the paper.
v^*	A fixed constant, 35.7 mV, from the *i/v* relationship of the light-sensitive current measured by Haynes and Yau (1985).
E	The reversal potential of the light-insensitive current, measured relative to the dark membrane potential.

significant contribution to the cone membrane potential. In fact, a computation reveals that one implication of this electrogenicity is that about one-third of the inward light-sensitive current in the steady state must return outward via the Na^+/K^+ exchange pump; this is mandated by charge balance and mass balance for Na^+, K^+ and Ca^{2+}. If the hyperpolarizing current from the Na^+/K^+ exchange pump decays slowly to zero after the light-sensitive current is shut off (as it must to achieve a steady state for $[Na^+]_i$), this current provides another feedback process which opposes the direct effect of light on the cone membrane potential.

We found that we could not account for the shallowness of the steady-state cone membrane potential as a function of I_0 without including electrogenic Na^+/K^+ exchange in the model. With this Na^+/K^+ pump the model cone hyperpolarizes ~4 mV per log unit of light, in the regime where the logarithmic approximation holds (see above), instead of ~7 mV when the pump is ignored. Furthermore, when this pump is included, the dark-adapted intensity-response function is well approximated by the Naka–Rushton equation; but when the pump is ignored, the intensity-response function is much too shallow.

Following Sneyd and Tranchina (1989) the kinetic equation for $[Ca^{2+}]_i$ can be written as

$$B_o \frac{d}{dt}(\Omega[Ca^{2+}]_i) = \frac{\epsilon}{2F} K x^n e^{-V/v^*} - \alpha_1[Ca^{2+}]_i, \qquad (13)$$

where $-Kx^n e^{-V/v^*}$ is the total light-sensitive current; $1 - \epsilon$ and ϵ are the fractions carried by Na^+ and Ca^{2+}, respectively (we ignore other current carriers); $\Omega[Ca^{2+}]_i$ is the total cytoplasmic concentration of Ca^{2+}; B_o is the volume of the outer segment; α_1 is the first-order rate constant for the Na^+/Ca^{2+}–K^+ exchange pump; F is Faraday's constant. If we assume that (*a*) Na^+ is not buffered in the cone and diffuses freely between outer and inner segment; (*b*) 4 Na^+ ions are pumped in for every Ca^{2+} out (Cervetto et al., 1989); (*c*) the Na^+/K^+ exchange pump obeys first-order kinetics (Torre, 1982) with rate constant ν_1, then the rate equation for Na^+ is

$$B_i \frac{d}{dt}[Na^+]_i = \frac{(1-\epsilon)}{F} K x^n e^{-V/v^*} - \nu_1[Na^+]_i + 4\alpha_1[Ca^{2+}]_i, \qquad (14)$$

where B_i is the total cone volume.

In the membrane-current conservation equation we must include capacitative current, light-sensitive current, current from the two exchange pumps, and outward current carried largely by K^+ through the inner-segment membrane. Thus, the membrane polarization V satisfies

$$C\frac{dV}{dt} = K x^n e^{-V/v^*} - \frac{F\nu_1}{3}[Na^+]_i - G(V - E) + F\alpha_1[Ca^{2+}]_i, \qquad (15)$$

where C is the membrane capacitance; G is conductance of the inner-segment membrane; E is the reversal potential for the light-insensitive current (measured relative to the dark resting potential).

If we use the definition $y = [Ca^{2+}]_i/[Ca^{2+}]_i^{dark}$ and define z similarly as $z = [Na^+]_i/[Na^+]_i^{dark}$, then Eqs. 13–15 can be written as

$$\frac{dy}{dt} = \alpha(x^n e^{-V/v^*} - y) \qquad (16)$$

$$\frac{dz}{dt} = \nu\left(\frac{1-\epsilon}{1+\epsilon}x^n e^{-V/v^*} - z + \frac{2\epsilon}{1+\epsilon}y\right) \qquad (17)$$

$$\tau_m \frac{dV}{dt} = -\left(\frac{6}{4+\epsilon}\right)Ex^n e^{-V/v^*} + 2\left(\frac{1+\epsilon}{4+\epsilon}\right)Ez - (V-E) - 3\left(\frac{\epsilon}{4+\epsilon}\right)Ey, \quad (18)$$

where $\alpha = \alpha_1/(B_o\Omega)$; $\nu = \nu_1/B_i$; and $\tau_m = C/G$. Note that all other parameters drop out of the equations because of the constraints that the dark steady state (where $z = 1, y = 1, V = 0$) puts on the relationships among the parameters. For example, Eq. 14 implies that $\alpha_1 = \epsilon K/(2F)$. In the new, modified model Eqs. 17 and 18 replace Eq. 9. As with the previous model (Sneyd and Tranchina, 1989), the steady-state constraint, Eq. 12, allows one to compute analytically the feedback function $g(y)$ and the steady-state relations $p_0(I_0)$, $x_0(I_0)$, $y_0(I_0)$, and $z_0(I_0)$.

In fitting the model to data, with a least-squares method (Sneyd and Tranchina, 1989), we use nine parameters which are variable from cell to cell: η, β, γ, α, τ_m, τ_1, k_1, k_2, and E. In fitting our previous model to the data (Sneyd and Tranchina, 1989), τ_1 and E were not allowed to vary from cell to cell, and the parameters k_1 and k_2 were determined by a separate fit of the low-frequency data. In fitting the present model, we used the same methods to set initial values of τ_1, E, k_1, and k_2, but then made small adjustments in these parameters to improve the fit and give intensity response functions closer to the required Naka–Rushton curves (see Results). A typical data set, Fig. 3 *a* for example, is a family of temporal frequency responses consisting of 88 data points, 44 amplitudes and 44 phases.

Effects of parameters on model behavior

Due to the complexity of the model, it is not possible in general to determine analytically the effect each of the model parameters has on behavior of the model. However, the effect of each parameter could still be determined by numerical simulations. The following comments may give additional insight. Making any one of the rate constants, β, γ, η, δ, smaller or either of the time constants, τ_1, τ_m, larger (while holding all other parameters fixed) will slow down the kinetics of the response. Gain of the temporal frequency response will fall more rapidly with increasing frequency, and phase lag of the response will increase more rapidly. The rate constant α plays a particularly important role in that it controls the time course of feedback under normal physiological conditions where $[Ca^{2+}]_i$ is free to vary. Making α smaller, while holding other parameters fixed, gives greater low-frequency attenuation in the temporal frequency response (see Fig. 3) and larger overshoot in the recovery phase of the impulse response (see Fig. 6). The parameter E determines the maximal response amplitude ($3E/2$) which could be obtained by suddenly reducing [cGMP] to zero.

Our method of determining model parameters by fitting linear-regime data alone does not pin down model parameters very tightly. There is some flexibility in the choice of parameters because change in one parameter can be compensated for by change in another. For heuristic purposes let us consider the gain and kinetics of the impulse response function, $q(t)$ in the simpler model of Sneyd and Tranchina (1989), under the simplifying conditions where $[Ca^{2+}]_i$ is held fixed at its dark level, to eliminate feedback. One measure of gain of the impulse response is area under its waveform, which under these conditions is given by $(\eta/\beta)(\gamma/\delta)(nE/[1 - E/v^*])$. The first moment of the normalized (to unit area) impulse response measures dispersion of the response. The first moment is given by $4\tau_1 + \beta^{-1} + \delta^{-1} + \tau_m/[1 - E/v^*]$. Thus, it is clear that the first moment and gain of the impulse response can be held more or less fixed if a change in one model parameter is compensated for by the appropriate change in another.

Finally, we note that one characteristic feature of light adaptation captured by the model, sensitivity inversely proportional to background light level, results from the nonlinear dependence of guanylate cyclase activity on $[Ca^{2+}]_i$. The particular form of the guanylate cyclase activity function is determined by constraining the steady-state voltage to follow Eq. 12.

METHODS

Preparation

Intracellular recordings were obtained from six red-sensitive cones in the isolated eyecup preparation of the turtle *Pseudemys scripta elegans*. The preparation and recording methods were similar to those described previously (Tranchina et al., 1983). The eyecup was placed in a recording chamber supplied with moistened O_2. A Peltier device, controlled by a feedback circuit (designed and built by Michelangelo Rossetto), maintained the temperature of the preparation at 18°C. The preparation, recording apparatus, and some optical components were located inside a Faraday cage in which the stray light from outside was well below any stimulus intensity used in our study.

Visual stimuli

We used a three-channel optical system. One channel contained a monochromator (H10; Instruments SA, Metuchen, NJ) used to measure spectral sensitivity. A second channel was used to present images displayed on a cathode ray tube oscilloscope (608 with P31 phosphor; Tektronix, Beaverton, OR). The images were generated by a computer-based visual stimulator (V-4; The Rockefeller University, Laboratory of Biophysics, and Electronics Shop, New York). The image on the CRT measured 100 × 100 mm and consisted of 256 × 256

picture elements; the frame rate was 270 Hz. The mean luminance of the CRT, measured with an optometer (61CRT; United Detector Technology, Hawthorne, CA), was 100 cd/m^2. The spatial capabilities of the visual stimulator (V-4) and CRT were used primarily to generate drifting sinusoidal gratings for measurement of spatial transfer functions (frequency responses). The CRT display was imaged onto the retina by a photographic lens (85 mm, f/1.4, Nikkor; Nikon, Garden City, NY); the object-to-image ratio was 16. The third optical channel contained a high-intensity red light-emitting diode (LED) (H500, Hi-Super Brite; Stanley, Tokyo, Japan). The LED was placed behind a diffuser at a distance of ~3 cm from the retina to obtain more or less spatially uniform light in the retinal plane. Use of spatially uniform illumination in the light adaptation studies serves to minimize lateral spread of current in the network of electrically coupled cones (Detwiler and Hodgkin, 1979). Its intensity was controlled by a feedback circuit (Michelangelo Rossetto). In this circuit, current to the LED was driven by the difference between two signals (i.e., error): one was a command signal from V-4, which controlled (temporal) contrast, and the other was an amplified signal from a homemade photomultiplier (Michelangelo Rossetto), which monitored the intensity of the LED. The gain of the photomultiplier signal was variable in steps of 0.3, 0.7, and 1.0 log units, over an entire range of 6 log units. For a given command signal, typically a sinusoidal waveform, the effect on retinal irradiance of increasing the gain of the photomultiplier signal by n log units was equivalent to inserting a neutral density filter of n log units between the LED and the retina. Thus, V-4 was used to control the contrast of the LED stimulus, and the mean light level was controlled by the feedback circuitry. The highest mean light level which could be delivered by the LED in this configuration was 7.2×10^{13} quanta s^{-1} cm^{-2}. Throughout the paper, light intensity I will be measured in relative units, where I equals physical intensity divided by 7.2×10^{13} quanta s^{-1} cm^{-2}. The highest mean level used in our study was a −0.3-log unit level (attenuation), i.e., a mean light level of 3.6×10^{13} quanta s^{-1} cm^{-2}. This light level reduced the flash sensitivity by a factor of ~100 from the dark-adapted level and bleached ~10% of the photopigment (estimated from the data and computations of Normann and Perlman, 1979). The lowest light level used gave ~20 photoisomerizations/s (estimated from the data and computations of Baylor and Hodgkin, 1973). The spectral distribution of light from the LED was measured with a spectrophotometer. The spectral peak was at 670 nm and 90% of the photons were in the 640–690 nm range.

Recording techniques and data storage

Recordings were obtained with microelectrodes pulled, from 1.0 mm O.D. glass pipettes (B100; World Precision Instruments, Inc. [WPI], New Haven, CT), on a Brown-Flaming micropipette puller (P-77B; Sutter Instrument Co., San Francisco, CA). Electrodes with resistances ~200 MΩ worked best. Intracellular signals were amplified with a WPI 707A amplifier and displayed on a storage oscilloscope (5103; Tektronix). Intracellular signals were further amplified (to range over −5–+5 V) and sampled, at the frame rate of V-4, by a 12-bit analogue-to-digital converter. The samples were stored in bins phased to the stimulus cycle and signal averaged for 15.2 or 30.4 s, depending on the temporal frequency. The signal-averaged response was displayed continuously during an experimental run. The response and stimulus parameters were stored in a file for later analysis off line.

Cell identification

Red-sensitive cones were identified by depth in the retina, waveform of the response, spectral sensitivity, and spatial sensitivity profile. Previous studies (Detwiler and Hodgkin, 1979; Copenhagen and Green; 1987) have shown that the spatial sensitivity profile of turtle cones is well described by an exponential line-weighting (line-spread) function. We identified cones by measuring the corresponding spatial frequency response at a fixed temporal frequency of 2.1 Hz. Cones can "resolve" high spatial frequencies. Some cones were identified by sampling only 2–3 points of their spatial frequency response which included 10 cycles/mm.

A spatial frequency response is defined by the amplitude and phase of the response to a drifting sinusoidal grating, measured as a function of spatial frequency and at a fixed temporal frequency. The stimulus is described by

$$I(x, t) = I_0[1 + m \sin (2\pi\zeta x - 2\pi ft)],$$

where ζ is spatial frequency (in cycles per millimeter on retina); m is contrast; f is temporal frequency or drift rate (measured in cycles per second); I_0 is mean light level. The spatial frequency response corresponding to the exponential line-weighting function (Tranchina et al., 1983) is of the form

$$T(\zeta) = \frac{c}{1 + [2\pi\zeta\lambda]^2}, \tag{19}$$

where c depends on the temporal frequency f of measurement, and λ is the exponential space constant of the corresponding line-weighting function.

For the cones in our study, λ ranged between 24–40 μm. Fig. 2 shows a typical spatial frequency response measured at 2.1 Hz. Data are plotted with symbols, and the continuous line is drawn from Eq. 19 with λ = 29 μm. Discrepancies between the experimental spatial frequency responses and Eq. 19 at low frequencies, like those shown in Fig. 2, were observed in 5 out of 12 cones in which we measured spatial frequency responses. Only 6 of these 12 cones provided complete light adaptation data and are included in this study.

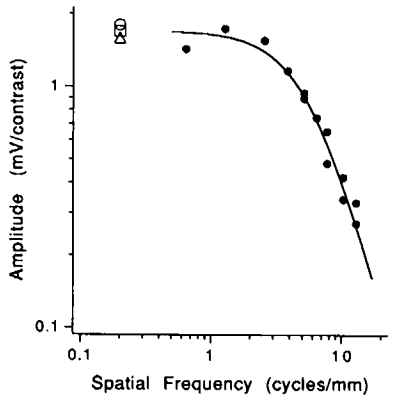

FIGURE 2 The spatial frequency response of a cone to drifting sinusoidal gratings with a fixed temporal frequency (drift rate) of 2.1 Hz. The filled circles give the experimental contrast gain (i.e., amplitude of the fundamental Fourier component of the response divided by grating contrast) as a function of spatial frequency, and the smooth curve is a plot of Eq. 19. The open circle and triangle are data points measured at zero cycles per millimeter (sinusoidal modulation of full-field illumination), and the open square is the corresponding theoretical value from Eq. 19.

RESULTS

Temporal frequency responses in theory and experiment

Temporal frequency responses were measured in the following way. A stimulus of the form

$$I(t) = I_0[1 + m \sin(2\pi ft)]$$

elicited a response of the form

$$v(t) = v_0 + v_1 \sin(2\pi ft + \theta_1) + v_2 \sin(2\pi 2ft + \theta_2) + \cdots$$

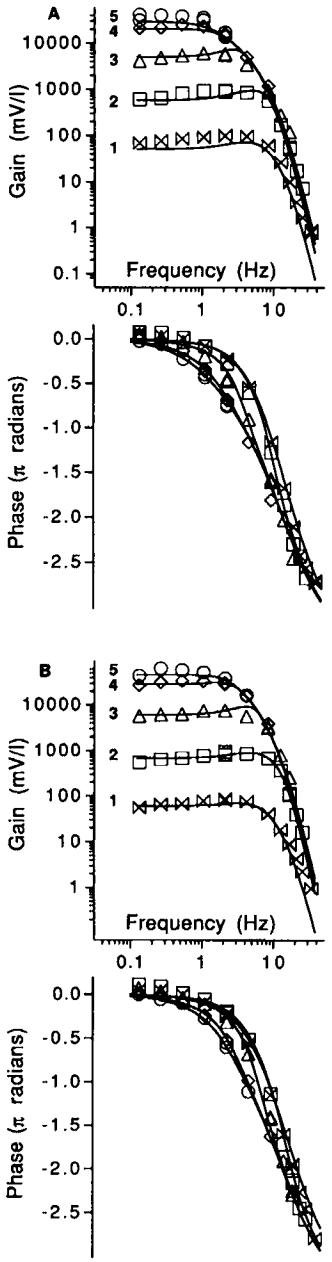

The contrast $m = (I_{max} - I_{min})/(I_{max} + I_{min})$ used to estimate the first-order frequency response was chosen such that the response contained little power in the Fourier components beyond the input (fundamental) frequency; the amplitude of the second-harmonic component of the response was $< 10\%$ of that of the fundamental. For high light levels, for example, m was 0.25 for frequencies below 16.9 Hz, whereas for frequencies $\geq$ 16.9 Hz, m was 0.5. The quantities v_1/mI_0 and θ_1 were determined by Fourier analysis and were used as estimates of the gain and phase of the first-order frequency response.

Fig. 3 *a* shows a family of temporal-frequency responses (*symbols*) from a red-sensitive cone, number 6 in Table 3. Measurements were made at five mean light levels separated by 1 log unit steps. Gain is plotted in the upper panel. Phase difference between input sinusoid and fundamental component of the response is plotted in the lower panel. The uppermost gain curve corresponds to the lowest light level, where the gain is greatest; the lowermost gain curve corresponds to the highest light level, where the gain is lowest. Fig. 3 *a* shows that, at each frequency, phase lag and gain of the response decreases with increasing mean light level. The solid lines in Fig. 3 *a* plot theoretical frequency responses from the model, with $\delta = 5\ s^{-1}$ and parameter values from Table 3. These and all computations in this paper were done from the full set of equations of the model including electrogenic Na^+/K^+ exchange, with the rate constant for Na^+ extrusion $\nu = 25\ s^{-1}$ (Torre, 1982). The behavior of the model over short time periods is very insensitive to ν when ν is on the order of several seconds. Fig. 3 *b* shows similar data from cell 5 with a somewhat better fit of the model compared with the fit for cell 6 in Fig. 3 *a*. The data in Fig. 3 *b* is the same as

FIGURE 3 (*A*) First-order frequency response of a cone (number 6 in Table 3). Gain and phase are shown in the upper and lower panels, respectively. The frequency response was measured at five background light levels. The uppermost gain curve corresponds to the lowest mean light level, and the lowermost gain curve corresponds to the highest mean level. The symbols are the experimental data, and the smooth curves are calculated using the best-fit values for the parameters. As in the text, the intensity I is measured in relative units. Therefore, to convert gain in this figure to physical units mV quanta^{-1} s cm^2, the gain values should be multiplied by 7.2×10^{13}. The smooth curves were calculated using the values of the parameters given in Table 3 (cone 6). The experimental mean light levels were (in relative units) 0.5, 0.05, 0.005, 0.0005, and 0.00005; they are labeled 1–5, respectively. Stimulus contrast was 0.25 for all frequencies, except those > 16 Hz, where the contrast was 0.5. At each mean light level, measurement of the frequency response began and ended with 2.1 Hz; for this frequency (and others which were repeated), the individual data points are plotted to show stability of the impalement and reproducibility of the measurements. (*B*) Similar data and fits for cone 5 (Table 3).

TABLE 3

Cone	Model parameters								
	k_1	k_2	E	τ_1	η	β	γ	α	τ_m
	mV	—	mV	s^{-1}	s^{-1}	s^{-1}	s^{-1}	s^{-1}	s
1	2.00	1980	−16	0.010	31.1	31.5	227	22.7	0.018
2	1.78	1970	−13	0.010	71.7	16.6	132	16.4	0.015
3	1.73	901	−12	0.014	54.8	51.6	363	15.7	0.019
4	1.71	1350	−14	0.012	66.2	72.7	568	23.1	0.014
5	1.86	1460	−16	0.012	167.0	40.6	252	16.2	0.016
6	1.59	1130	−13	0.012	52.5	35.4	298	13.5	0.016

These steady-state and dynamic parameters for the model (all but E) were determined by fitting the model to experimental data on the first-order temporal frequency response of turtle cones. The parameter E determines the maximal response amplitude of the model cone ($V_{max} \sim [3/2]E$). Details of the procedure are given in Sneyd and Tranchina (1989). Note that because voltages are expressed in dimensionless form by Sneyd and Tranchina, but not here, and because the present model includes electrogenic Na^+/K^+ exchange, the best-fit values for all the parameters change. Furthermore, the time constant in the voltage equation is defined differently in the two papers, so that the parameter τ_m in this table replaces τ in Sneyd and Tranchina (1989).

that in Fig. 2 of Sneyd and Tranchina (1989) but fit here with the new model.

The model provides a good fit to the data in which gain varies over more than four orders of magnitude. The fit of the model to data is not perfect, however; there is a small discrepancy between the model and experimental phases at high light levels and low frequencies, where the model does not give the small phase advance seen in the data. This was a consistent finding from cell to cell. Our hypothesis is that this discrepancy results from neglect of a time and voltage-dependent conductance mechanism in the inner segment membrane (Attwell et al., 1982; Barnes and Hille, 1989; Maricq and Korenbrot, 1990). Furthermore, the model fails to fit the data at the highest frequencies, at high light levels. We believe this discrepancy reflects the fact that our model of the initial stages of transduction leading up to the production of activated G-protein is not correct in detail. Similar data and fits were obtained on all six cells. Frequency responses were measured at five levels of I_0 for four cones, and at only four levels for cones 3 and 4 (Table 3). The best-fit values for the model's parameters for each cell are given in Table 3.

Robustness of the model

Computations show that, in a region close to the best-fit parameter values, the first-order frequency response is not very sensitive to the parameter values; consequently, precise values for the parameters cannot be obtained. We have found that changing any of the best-fit parameters by ±20% resulted in ~10% change in the error function. This makes little difference to the fit and is hardly noticeable in the theoretical frequency responses. This feature is actually desirable, as it indicates stability of the model: similar behavior can be obtained by a range of parameter values, and thus the properties of the model are not dependent on the precise values obtained by the fit.

Guanylate cyclase activity

The dependence of guanylate cyclase activity on $[Ca^{2+}]_i$ inferred from fitting the model to experimentally measured frequency responses is shown in Fig. 4 *a* (*solid line*). Note that cyclase activity in Fig. 4 *a* is measured in the units indicated in Table 1. As $[Ca^{2+}]_i$ decreases from its value in the dark, the activity of guanylate cyclase rises along a sigmoidal curve. For the particular cell in Fig. 4 (the same cell used in Fig. 3 *a*), the value of guanylate cyclase activity at a relative Ca^{2+} concentration of 0.24, obtained at the highest light level in our study, is ~15 times that in the dark. At even lower values of $[Ca^{2+}]_i$ (not plotted in Fig. 4 *a*) cyclase activity rises to a peak value which is 20 times its dark value. The dashed curve in Fig. 4 *a* is plotted from the equation

$$A(y) = A_{min} + \frac{A_{max} - A_{min}}{1 + (y/Y)^m}, \qquad (20)$$

(Pugh and Lamb, 1990). The function $A(y)$ in Eq. 20 is the dependence of the rate of synthesis of cGMP on $[Ca^{2+}]_i$ that is suggested by the experimental results of Koch and Stryer (1988). In Eq. 20, A_{max} is the maximal rate, which is approached as $[Ca^{2+}]_i$ approaches zero; A_{min} is the minimum rate at high values of $[Ca^{2+}]_i$; y is $[Ca^{2+}]_i$, measured in relative units (see Table 1); and Y is the value of $[Ca^{2+}]_i$ that gives half the maximal change in cyclase activity; m is the Hill coefficient for the cooperative inhibition of cyclase activity by Ca^{2+}. In the plot of Eq. 20 (Fig. 4 *a*) $A_{max} = 95$; $A_{min} = 4$; $Y = 0.34$; $m = 4$. These values were chosen to give a good match between the cyclase activity predicted by our model and that given by Eq. 20. The good overall agreement between the solid and dashed curves is quantitative evidence that a functional dependence of cyclase activity on $[Ca^{2+}]$ like that reported by Koch and Stryer (1988) for bovine rods is indeed sufficient to account for light adaptation in turtle cones. It is important to emphasize that Fig. 4 *a* makes a comparison between the dependence of cyclase activity on $[Ca^{2+}]_i$ in the model and the *functional form* suggested by the results of Koch and Stryer (1988); we are not comparing absolute values of cyclase activity at absolute values of calcium concentration. Nevertheless, the 20-fold increase in cyclase activity from dark to bright light in our model is consistent with the 5 to

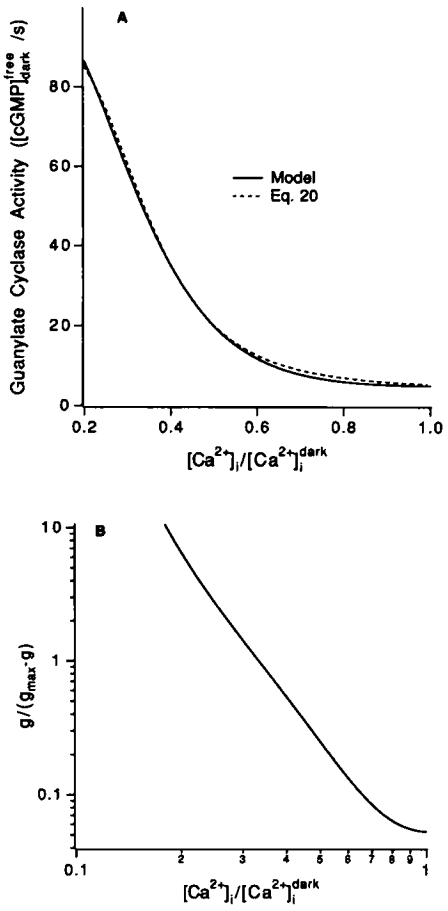

FIGURE 4 (*A*) A plot of the theoretical dependence of guanylate cyclase activity, g, on $[Ca^{2+}]_i$ according to the model (*solid curve*). "Guanylate cyclase activity" is defined here as the rate of production of cGMP by guanylate cyclase and is measured in units of $[cGMP]^{free}_{dark}$ s^{-1}. The solid curve was calculated using the best-fit values for the parameters from cone 6 (Table 3). The dashed curve is plotted from Eq. 20 with $A_{max} = 95$, $A_{min} = 4$, and $Y = 0.34$. (*B*) Hill plot of guanylate cyclase activity of the model corresponding to the solid curve in part *A*. The lowest value of $[Ca^{2+}]_i$ plotted, $[Ca^{2+}]_i/[Ca^{2+}]_i^{dark} = 0.2$ is somewhat lower than the value of 0.24 achieved at the highest light level in our study according to the model.

20-fold dynamic range of cyclase activity found by Koch and Stryer (1988). Furthermore, the Hill coefficient (m) of 4 which we used in the plot of Eq. 20 (Fig. 4 *a*) is the average value reported by Koch and Stryer (1988).

Fig. 4 *b* is a Hill plot of guanylate cyclase activity of the model corresponding to the solid curve in Fig. 4 *a*. This Hill plot is similar to that obtained in the experiments of Koch and Stryer (1988), illustrated in their Fig. 1 *b*.

Similar results were obtained in all cells. The precise shape of the guanylate cyclase function in the model depends to some extent on the assumed value of activity in the dark. As pointed out by Sneyd and Tranchina (1989), the fit of the model to our adaptation data is not very sensitive to this parameter. From a number of computations (not shown), it appears that, in the model, a lower assumed dark rate does not change the peak rate much and therefore gives a larger ratio of peak to dark guanylate cyclase activity.

Dependence of $[Ca^{2+}]_i$, [cGMP], and [PDE*] on I_0

The steady-state values of $[Ca^{2+}]_i$, [cGMP], and [PDE*] are plotted in relative units vs. steady light level in Fig. 5. In this figure the concentrations $[Ca^{2+}]_i$ and [cGMP] are measured relative to their dark values, and [PDE*] is measured relative to the total concentration of phosphodiesterase (activated plus inactivated). The curves were computed from the model equations, with parameters from the cell in Fig. 3 *a*. The highest steady light level used in our study was 0.5 (−0.3 log unit level), measured in relative units. Fig. 5 demonstrates a shallow dependence of $[Ca^{2+}]_i$ and [cGMP] on I_0, and a relatively steeper dependence of [PDE*] on I_0. At the −0.3 log unit light level, where low-frequency gain is decreased by a factor of ~1,000 from the dark-adapted value (see Fig. 3 *a*), [cGMP] has decreased by only ~40%, and $[Ca^{2+}]_i$ by ~80% from their dark levels; in contrast, by inspection of Figs. 4 and 5, guanylate cyclase activity has increased ~18 times from its dark value.

From Fig. 5 we may conclude that, under normal physiological conditions, depletion of cGMP plays little

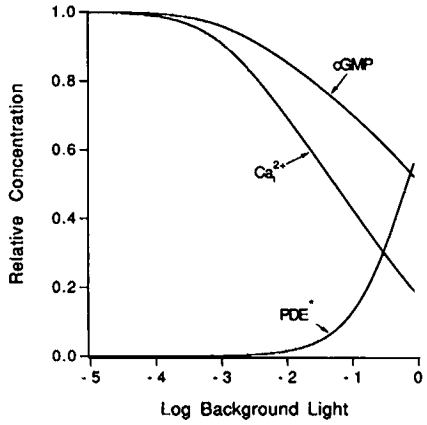

FIGURE 5 Steady concentrations of activated phosphodiesterase (p), free cytoplasmic calcium (y), and free cGMP (x), vs. the steady background light level (I_0). The concentrations $[Ca^{2+}]_i$ and [cGMP] are measured relative to their dark values, and [PDE*] is measured relative to the total phosphodiesterase concentration (cf. Table 1). These were calculated from the model using the parameters from cone 6 (Table 3). These functions were computed from the steady-state solutions of the model equations (cf. Sneyd and Tranchina, 1989).

role in the reduction of sensitivity over the range of experimental light levels in our study. We show later in the paper that the picture is quite different when Ca^{2+} feedback is removed. Furthermore, because PDE* is far from saturation over the four lowest light levels, saturation of PDE* plays little role in reduction of response gain over these light levels. At the highest light level, on the other hand, saturation of PDE* does become important.

Impulse response

Contrast sensitivity, kinetics, and time to peak

For the sake of comparing the behavior of the model to the experimental results of others, Fig. 6 shows a family of impulse response functions of the model for flashes of fixed contrast superimposed on various background light levels (i.e., $Q/I_0 = k$, where Q is the total number of photons in the flash superimposed on the background light level I_0, and k is a constant). The background levels are from the set of the mean light levels in Figs. 3, *a* and *b*. Linear-regime responses were computed by solving the differential equations of the model and checking that the response scaled with input. In Fig. 6 *a* the response at the lowest experimental light level is omitted for the sake of figure clarity, but it is plotted on a different scale, along with the response for the next-lower level, in Fig. 6 *b*. In Figs. 6, *a* and *b*, incremental responses $[V(t) - V_0(I_0)]$ are plotted to show changes in response kinetics and contrast sensitivity with I_0. One measure of contrast sensitivity is given by the peak amplitude of the cone's flash response divided by the contrast of the flash. Figs. 6, *a* and *b*, show that the contrast sensitivity of the impulse response, given by the model cone, increases as the background light level increases, up to a point, and then decreases again. Thus, the contrast sensitivity of the model cone (which simply reflects that measured experimentally in the frequency domain) is consistent with previous results of Baylor and Hodgkin (1974, Fig. 2), Daly and Normann (1985, Fig. 4), and Naka et al. (1987, Fig. 5). For half the cones in our study, the contrast sensitivity at the −0.3 log unit level was less than that at the −1.3 log unit level. A decrease in (impulse response) contrast sensitivity at high light levels has been measured previously by Daly and Normann (1985). The contrast sensitivity given by our model, for every parameter set in Table 3, first increases and then decreases with background light level; where the "turnaround" occurs depends on the model parame-

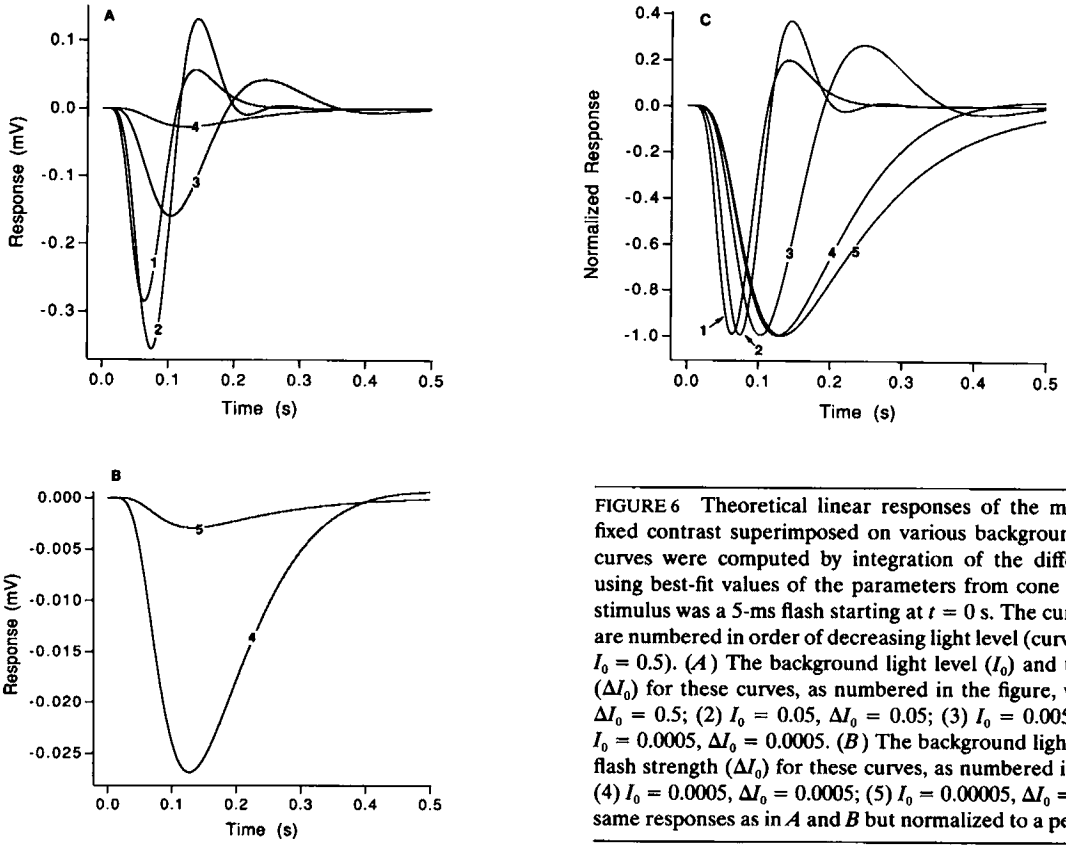

FIGURE 6 Theoretical linear responses of the model to flashes of fixed contrast superimposed on various background light levels. All curves were computed by integration of the differential equations using best-fit values of the parameters from cone 6 (Table 3). Each stimulus was a 5-ms flash starting at $t = 0$ s. The curves in *A*, *B*, and *C* are numbered in order of decreasing light level (curve 1 corresponds to $I_0 = 0.5$). (*A*) The background light level (I_0) and the flash strengths (ΔI_0) for these curves, as numbered in the figure, were: (1) $I_0 = 0.5$, $\Delta I_0 = 0.5$; (2) $I_0 = 0.05$, $\Delta I_0 = 0.05$; (3) $I_0 = 0.005$, $\Delta I_0 = 0.005$; (4) $I_0 = 0.0005$, $\Delta I_0 = 0.0005$. (*B*) The background light level (I_0) and the flash strength (ΔI_0) for these curves, as numbered in the figure, were: (4) $I_0 = 0.0005$, $\Delta I_0 = 0.0005$; (5) $I_0 = 0.00005$, $\Delta I_0 = 0.00005$. (*C*) The same responses as in *A* and *B* but normalized to a peak value of −1.

ters. For half the cells in Table 3, the model gives a turnaround at mean light levels greater than the highest level used in our study.

In Fig. 6 *c*, the normalized impulse response functions for all five experimental light levels are plotted again to show more clearly how the kinetics depend on background light level. The impulse response of the model is monophasic at the −4.3 log unit background light level, and the time to peak is 129 ms. As the background light level increases the impulse response becomes biphasic, and the time to peak becomes shorter; at the −0.3 log unit light level the time to peak is 64 ms.

Time to peak at the −4.3 log unit level ranged between 116 and 158 ms for the set of six cells in our study, while that at the −0.3 log unit level ranged between 49 and 72 ms (cf. Fig. 5 in Sneyd and Tranchina 1989).

Linearity of the incremental response

An important test of a model for phototransduction is provided by examining the extent of linearity of the response. Because there are numerous nonlinearities in the system of differential equations describing the model, the degree of linearity of the response cannot be anticipated a priori.

A remarkable feature of turtle cones and horizontal cells is that they respond quite linearly to moderate perturbations in light around a mean level (Tranchina et al., 1981; Chappell et al., 1985; Daly and Normann, 1985; Naka et al., 1987). A perfectly linear, time-invariant input-output system responds to a sinusoidal input with a sinusoidal output at the input frequency. Nonlinearities result in frequency components in the output at integer multiples (harmonics) of the input frequency. One index of nonlinear distortion is given by the ratio of second harmonic to first harmonic (fundamental) amplitudes. This measure is reasonable for moderate-contrast stimuli because they elicit practically no response components at the third and higher harmonics. The nonlinearity index of the model is similar to that measured experimentally at each light level. For example, at a relative light level of 0.5 (the highest level used), the range of the nonlinearity index, for eight frequencies between 0.132 and 16.9 Hz, was 2–8%, and the mean was 5%; the corresponding range for the model was 1–9%, and the mean was 6%. For lower light levels, the nonlinearity index decreases both for the experimental data and the model. Thus, our model for phototransduction does satisfy the requirement that it behave sufficiently linearly.

Shift of the V-log I curve with adaptation

An important summary of some aspects of light adaptation in turtle cones is provided by a family of intensity-response functions, at various background light levels, as measured by Normann and Perlman (1979). They found that plotting the peak membrane polarization (measured from the dark membrane potential, v_{dark}), in response to a step of light, versus the log of the step intensity (log I) gave a sigmoidal curve. To a first approximation, the effect of a steady background illumination on the peak polarization to a superimposed step was to shift the dark-adapted curve (i.e., the curve obtained with no background illumination) horizontally on the log I axis. Bright backgrounds caused a small vertical shift as well. Fig. 7 shows that the model gives shifting V-log I curves (*solid lines*) with background light. Normann and Perlman (1979) found their experimental intensity-response curves were fit by the Naka-Rushton equation

$$V = V_{max} \frac{I}{\sigma_N + I}, \tag{21}$$

where I is the light step intensity; σ_N is the light intensity that gives half the maximal response. The dashed curve in Fig. 7 is a plot of Eq. 21 with $V_{max} = -19$ mV and $\sigma_N = 1.28 \times 10^{-2}$, and it provides a fairly good fit to the model curve at the lowest light level. A flaw in the model is indicated by the fact that the theoretical intensity-response curves become progressively shallower as I_0

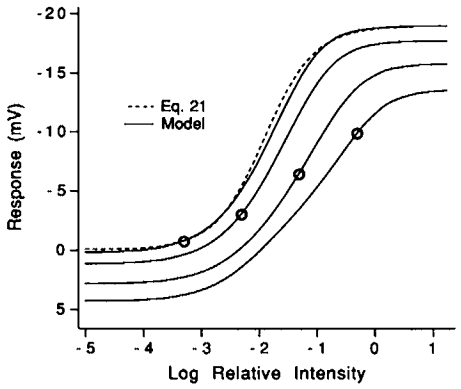

FIGURE 7 Theoretical intensity-response curves (*solid lines*) calculated from the model (parameters from cone 6 [Table 3]). The intensity-response curves in the figure correspond to the background light intensities (from left to right) 0.0005, 0.005, 0.05, and 0.5 (relative units). The steady voltage response for each of these background light levels is denoted by a symbol on the curve. The dashed curve is a plot of the Naka-Rushton equation (Eq. 21) where $\sigma_N = 1.28 \times 10^{-2}$ was chosen so that the curve goes through the point (V_0, I_0).

increases. In addition, for three out of six cells, the dark-adapted intensity response curve, according to the model, was shallower than the Naka-Rushton equation (with maximal discrepancies of 2.5–4 mV).

It is interesting to note that we found that the response of the original Sneyd and Tranchina (1989) model (which neglects Na^+/K^+ exchange) to a negative step of light has little if any overshoot for large negative steps and does not produce shifting V-log I curves. Choosing a steeper i/v relationship for i_{Ca} in the original model does give shifting intensity response curves, but they are always far too shallow.

Sensitivity with fixed and normal $[Ca^{2+}]_i$

Fig. 8 shows a simulation of an experiment of Matthews et al. (1988, 1990). Photocurrent sensitivity of the model (parameters from cell 6) was measured for linear-regime flash responses for various background light levels, (*a*) under normal conditions (*upper solid curve*); (*b*) with $[Ca^{2+}]_i$ fixed at the dark level (*lower solid curve*). The dashed line near the curve for normal conditions is the flash sensitivity S_F according to the Weber-Fechner relation

$$S_F/S_F^D = \frac{1}{1 + I_0/\sigma_W}, \tag{22}$$

(with $\sigma_W = 7.33 \times 10^{-3}$), where S_F^D is the flash sensitivity in darkness; I_0 is the background light level; and σ_W is the light level that reduces sensitivity to half its maximal value. The dashed line near the curve for the fixed Ca^{2+} condition is the curve used by Matthews et al. (1990) to fit sensitivity in salamander cones under conditions designed to fix $[Ca^{2+}]_i$ at its dark level:

$$S_F/S_F^D = \frac{1}{(1 + I_0/\sigma_M)^4}, \tag{23}$$

with $\sigma_M = 2.02 \times 10^{-2}$.

The dramatic steepening of the sensitivity curve for condition *b* appears to be caused by depletion of cGMP. Fig. 9 shows a graph of [cGMP] in the steady state as a function of background light level (*a*) under normal conditions (*dashed line*) and (*b*) with $[Ca^{2+}]_i$ fixed at the dark level (*solid line*), calculated from the model. It appears that when guanylate cyclase activity is frozen at its dark level, cGMP gets quickly depleted with increasing background light, owing to increasing [PDE*]. Thus, under these conditions, sensitivity falls because of a saturation nonlinearity.

Intensity-response function with fixed $[Ca^{2+}]_i$

One of the hallmarks of adaptation is that the intensity-response function becomes progressively more shallow with time after onset of a step of light. Nakatani and Yau (1988) showed that this signature of adaptation is absent when Ca^{2+} feedback is removed by fixing $[Ca^{2+}]_i$ at its dark level. Fig. 10 shows a simulation of their experiment. The normalized photocurrent response to a step of light is plotted (Fig. 10) as a function of step intensity at three different times (model parameters for cone 6).

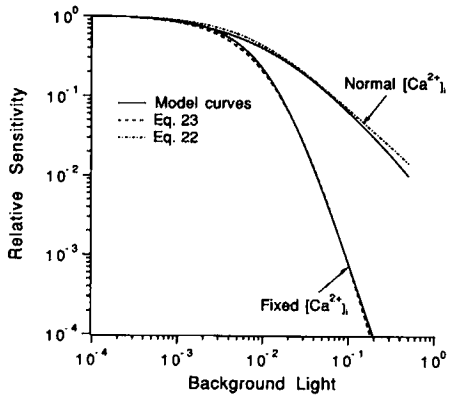

FIGURE 8 Incremental sensitivity as a function of background light intensity. Sensitivity is measured relative to the sensitivity in darkness. Computations are for linear-regime responses of the model to flashes superimposed on various background light levels, under two different conditions: (*a*) normal, i.e., $[Ca^{2+}]_i$ was left free to vary (*shallow solid curve*); (*b*) background light presented after $[Ca^{2+}]_i$ is fixed at its dark level (*steep solid curve*). The dashed curve near the curve for condition *a* is a plot of the Weber-Fechner function, Eq. 22 with $\sigma_W = 7.33 \times 10^{-3}$; the dashed curve near the curve for condition *b* is the polynomial curve, Eq. 23, with $\sigma_M = 2.02 \times 10^{-2}$.

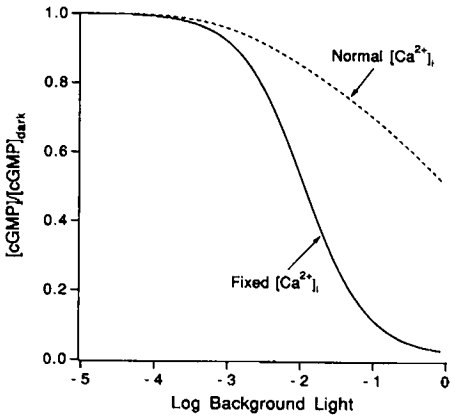

FIGURE 9 Steady-state [cGMP] as a function of steady light intensity under normal conditions (i.e., $[Ca^{2+}]_i$ was left free to vary) (*dashed curve*) and under conditions where the steady light is applied after fixing $[Ca^{2+}]_i$ at its dark level (solid curve).

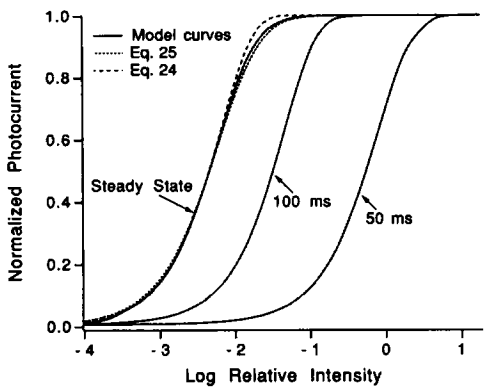

FIGURE 10 Intensity-response curves for the photocurrent given by the model (cone 6) under conditions where $[Ca^{2+}]_i$ is fixed at its dark level (Ca^{2+} feedback removed). The three solid curves, from left to right, correspond to the steady-state, 100 ms after the onset of the step, and 50 ms after step onset. The long-dashed curve is drawn according to Eq. 24 with $k = 1.5 \times 10^2$, and the short-dashed curve according to Eq. 25 with $\sigma_M = 1.8 \times 10^{-2}$.

The three solid curves, from left to right, correspond to the steady state, 100 ms after onset of the step, and 50 ms after step onset. When the response is measured at a fixed time, t_0, after the onset of the step, the intensity-response curve of the model is well approximated by a template curve shifted horizontally by an appropriate amount along the log I_0 axis (Fig. 10); as t_0 decreases, the intensity-response curve is shifted further to the right. This behavior of the model is in agreement with the results of Nakatani and Yau (1988).

The long-dashed curve in Fig. 10 is plotted from the equation (Nakatani and Yau, 1988)

$$\hat{i} = 1 - e^{-kI}, \tag{24}$$

where $\hat{i}$ is the normalized photocurrent; k is a constant (1.5×10^2); and I is the step intensity in relative units. The model curves conform reasonably well to Eq. 24. However, the model curves are described even better by the polynomial saturation curve used by Matthews et al. (1990) to fit intensity-response functions of salamander cones under conditions designed to hold $[Ca^{2+}]_i$ fixed at its dark level:

$$\hat{i} = 1 - (1 + I/\sigma_M)^{-3}. \tag{25}$$

The short-dashed curve in Fig. 10 is a plot of Eq. 25 with $\sigma_M = 1.8 \times 10^{-2}$. Note that this value of σ_M used in the steady-state intensity-response plot (Fig. 10, Eq. 25) differs by 0.05 log units from the value of σ_M used in the sensitivity plot (Fig. 8, Eq. 23). We show below that the condition for the two values of σ_M to be the same is for the integration time t_i to be fixed with I_0. The integration time is defined as the time integral of the impulse response function divided by its peak amplitude (Baylor and Hodgkin, 1973). We preface the proof below by emphasizing that the integration time t_i and the time to peak t_{peak} of the impulse response function are not necessarily correlated. If two impulse response functions have the same t_{peak} and peak amplitude, their t_i values will still differ if one response decays more rapidly than the other.

The claim that the two values of σ_m in Eq. 23 and 25 will be the same only if t_i is constant and independent of I_0 can be proven as follows. If we define $h(t; I_0)$ as the single-photon impulse response function at a background light level of I_0, then the response $\Delta r(t)$ to a small perturbation $\Delta I(t)$ superimposed on I_0 will be given by $\Delta r(t) \approx \int_{-\infty}^{t} \Delta I(t')\, h(t - t')\, dt'$, where the approximation is better the smaller is $\Delta I(t)$. If $\Delta I(t) = \Delta I_0$, a small steady perturbation, then the steady response pertubation Δr_0 is given by $\Delta r_0 \approx \int_0^\infty \Delta I_0\, h(t; I_0)\, dt$. Therefore, $\Delta r_0/\Delta I_0 \approx \int_0^\infty h(t; I_0)\, dt$. Passing to the limit as $\Delta I_0 \to 0$ gives $dr_0/dI_0 = \int_0^\infty h(t; I_0)\, dt$. If we use $h_{peak}(I_0)$ to denote $h(t_{peak}; I_0)$, then by definition $\int_0^\infty h(t; I_0)\, dt = h_{peak}(I_0)\, t_i(I_0)$. But $h_{peak}(I_0)$ is the peak response amplitude per photon, i.e., $h_{peak}(I_0) = S_F(I_0)$. Therefore, $dr_0/dI_0 = S_F(I_0)t_i(I_0)$. This means that when t_i is independent of I_0, the flash sensitivity $S_F(I_0)$ will be proportional to the derivative of the steady-state input-output function, dr_0/dI_0.

While it is true that t_{peak} of the model's impulse response varies little with I_0 when $[Ca^{2+}]_i$ is held fixed, t_i does become systematically shorter with increasing I_0. In computations not shown, we found that when $[Ca^{2+}]_i$ is frozen at its dark level in the model, t_{peak} of the impulse response decreases by only 10% at a value of I_0 where the light-sensitive current is already 90% saturated. However, under the condition of fixed $[Ca^{2+}]_i$, t_i becomes shorter with increasing I_0, despite the relative constancy of the time to peak, because of the increasingly more rapid decay of the impulse response function from its peak. This is demonstrated in Fig. 11 which shows normalized photocurrent impulse response functions for flashes superimposed on four different background light levels separated by one log unit step, where the lowest light level is $I_0 = 5 \times 10^{-5}$ (relative units). The normalized integration times (t_i divided by its dark value t_i^D) for the flash responses in Fig. 11 are 1, 0.97, 0.78, and 0.40, from the lowest to the highest value of I_0. The corresponding normalized flash sensitivities, S_F/S_F^D, are 1, 0.9, 0.4, and 0.007.

Analysis of the linearized equations of the model, which describe responses to small perturbations around a steady state, indicate that the change in response kinetics with I_0 illustrated in Fig. 11 stems mainly from the nonlinear term in the kinetic equation for cGMP

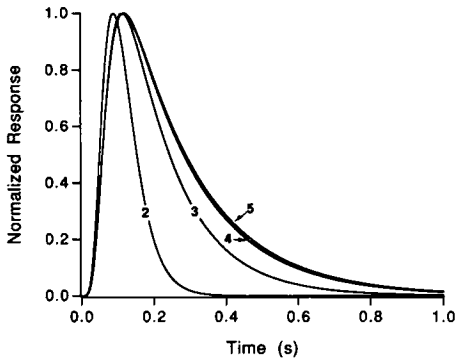

FIGURE 11 Normalized photocurrent impulse response functions of the model under the condition where $[Ca^{2+}]_i$ was held fixed at its dark level. The four responses correspond to flashes superimposed on the background levels (numbered as in Figs. 3 and 6) of (2) 5×10^{-2}, (3) 5×10^{-3}, (4) 5×10^{-4} and (5) 5×10^{-5}. Responses were computed by integration of the model's differential equations with y held fixed at $y = 1$.

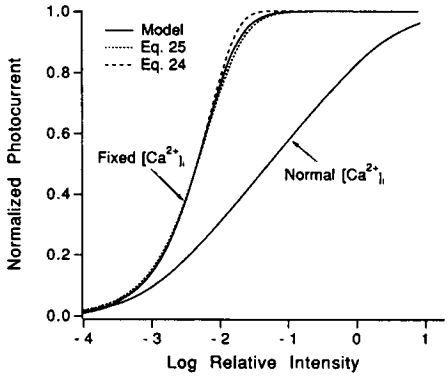

FIGURE 12 Normalized steady photocurrent versus light intensity (I_0) computed from the model under normal conditions (*shallow solid curve*), and under conditions where $[Ca^{2+}]_i$ is fixed at its dark level (*steep solid curve*). The long-dashed curve is drawn from Eq. 24, and the short-dashed curve from Eq. 25 with the same parameter values as in Fig. 10.

(Eq. 7) in which the concentrations of cGMP and PDE* are multiplied (see Discussion). The nonlinearity in the equation for membrane voltage (Eq. 18) makes less of a contribution.

Eq. 24 has been interpreted in various different contexts to suggest that the response is the probabilistic sum of the individual responses of numerous independent compartments, where there is complete channel closure within each compartment (Lamb et al., 1981; Baylor et al., 1984). Therefore, it is interesting that the intensity-response curves of the model, which has no compartments, follow Eq. 24 to a good approximation. The reason for the steep, approximately exponential saturation curve in the model has to do with the fact that the Hill coefficient n for the interaction of cGMP with the light-sensitive channel is > 1 (Matthews et al., 1990). Examination of the steady-state dependence of the light-sensitive current on I_0, for example, shows that it is approximately given by a quotient of polynomials in I_0, both of order n. This result is obtained by solving the equations of the model in the steady state, with the approximation $e^{-V/v^*} \approx 1 - V/v^*$. This quotient of polynomials provides a good approximation to the exponential saturation curve (Eq. 24) and the polynomial saturation curve (Eq. 25) of Matthews et al. (1990).

Fig. 12 shows results of model computations that simulate the experimental results of Matthews et al. (1990) showing the dramatic steepening of the steady-state intensity-response function when $[Ca^{2+}]_i$ is held fixed at its dark level. The shallow solid curve (Fig. 12) was computed (parameters from cell 6) for normal conditions (i.e. $[Ca^{2+}]_i$ left free to vary), and the steep solid curve was computed with $[Ca^{2+}]_i$ held fixed at its dark level. The long-dashed curve is plotted from Eq. 24, and the short-dashed curve is plotted from Eq. 25 (with the same parameters as in Fig. 10).

DISCUSSION

Summary

In a previous paper (Sneyd and Tranchina, 1989) we showed that a chemical kinetic model for phototransduction in cones accounts for the changes in gain and kinetics of red-sensitive turtle cone responses with light adaptation. Here we have put an extended version of this model to additional tests by simulating experiments in the literature. The chemical kinetic model accounts for the transition from a monophasic to a biphasic impulse response function with an increasing level of background illumination, and also accounts quantitatively for the dramatic decrease in response sensitivity with light adaptation. The extent of linearity of the incremental/decremental response of the model is consistent with experimental data. The model gives shifting of the $V - \log I$ curve (intensity-response function) with background light level (Normann and Perlman, 1979), although the model curves for high background light levels are more shallow than the Naka-Rushton equation (Eq. 21). In addition, the model simulates the contrasting behavior of photoreceptors with fixed and normal $[Ca^{2+}]_i$, measured in several different experiments by Matthews et al. (1988, 1990) and Nakatani and Yau (1988).

In the model, adaptation is achieved largely through a sigmoidal dependence of guanylate cyclase activity on

$[Ca^{2+}]_i$. This statement is based on examination of the analytical expression for the model's frequency response parametric in background light level I_0 (not shown), which is quite similar to that derived for our previous model that neglected electrogenic Na^+-K^+ exchange (Sneyd and Tranchina, 1989). Over the range of light levels used in our study, we find that the main determinant of gain and kinetics at each value of I_0 is the slope of the function giving cyclase activity as a function of $[Ca^{2+}]_i$, evaluated at the mean level of $[Ca^{2+}]_i$ established by I_0, i.e., $g'(y_0(I_0))$. If the sigmoidal guanylate cyclase activity function were replaced by a linear function, the slope would be constant with I_0, and the feedback would provide no adaptation at all. Instead, all changes in gain and kinetics would arise as a consequence of saturation nonlinearities. The depletion of cGMP, by itself, would cause sensitivity to fall off like the fourth power of I_0 as shown by us above and also by Matthews et al. (1990). It can also be shown that the saturation of PDE* would cause sensitivity to fall off like the square of I_0.

In our model, guanylate cyclase activity rises along a sigmoidal curve as $[Ca^{2+}]_i$ decreases from its dark value. The peak value of cyclase activity in the model is ~20-fold higher than its dark value, $[Ca^{2+}]_i^{dark}$. The dynamic range of cyclase activity in the model is sensitive to the assumed rate of cGMP turnover in the dark, δ, which is unknown for cones. The peak rate of cyclase activity, on the other hand, is not very sensitive to δ. Therefore, if we choose a value for δ which is twice as large, the predicted dynamic range for cyclase activity becomes about half as large. In the model the peak in cyclase activity is reached at $\sim 0.1 \times [Ca^{2+}]_i^{dark}$. According to the model, the second-highest light level corresponds to a steady value of $[Ca^{2+}]_i$ equal to $\sim 0.5 \times [Ca^{2+}]_i^{dark}$, and the highest light level to $\sim 0.2 \times [Ca^{2+}]_i^{dark}$. The dynamic range of cyclase activity in the model is on the high end of what Koch and Stryer (1988) found for cyclase activity in bovine rods. However, the range of calcium concentrations over which cyclase activity varies from minimum to maximum seems to be about the same in our model and in the experimental results illustrated in Fig. 1 of Koch and Stryer (1988). According to our model, the change in cyclase activity is half maximal at $[Ca^{2+}]_i \approx (1/3) \times [Ca^{2+}]_i^{dark}$. Koch and Stryer found that the change in cyclase activity in their bovine rod preparation was half maximal at a calcium concentration of ~90 nM. If we assume, for the sake of argument, that 90 nM is $\sim(1/3) \times [Ca^{2+}]_i^{dark}$ in bovine rods, then we would predict a value of $[Ca^{2+}]_i^{dark}$ of 270 nM in this preparation. We do not know the value of $[Ca^{2+}]_i^{dark}$ in bovine rods, but the figure of 270 nM does not seem unreasonable in light of the fact that $[Ca^{2+}]_i^{dark}$ in bullfrog rods has been estimated to be ~220 nM (Ratto et al., 1988). Despite the broad similarities between our model and rod physiology reported in the literature, there may be an important difference. According to the measurements of Ratto et al. (1988), bright light decreases $[Ca^{2+}]_i$ in bullfrog rods form a dark value of ~220 nM to ~140 nM in bright light. This dynamic range of $[Ca^{2+}]_i$ is not nearly as wide as that in our model. However, it is worth noting that the study of Cervetto et al. (1989) on the stoichiometry and voltage dependence of Na^+/Ca^{2+}-K^+ exchange in salamander rods gives a biophysical argument that $[Ca^{2+}]_i$ may drop to as low as 18 nM in this preparation.

By showing that cooperative inhibition of guanylate cyclase activity by Ca^{2+}, like that measured by Koch and Stryer (1988), is sufficient to account for changes in sensitivity and kinetics with background light level, our model lends quantitative support to the calcium feedback hypothesis for light adaptation. That is not to say that other mechanisms are excluded (see below).

We point out that nonlinear feedback in the model does not cause response kinetics to speed up indefinitely. This is reflected in the fact that the impulse response functions corresponding to light levels 1 and 2 (Figs 6, *a* and *c*) have similar waveforms. Over the range of high light levels in which adaptation is determined by nonlinear feedback, and before saturation nonlinearities come into play, the impulse response function more or less scales with I_0 without major changes in response kinetics. This type of behavior has been described quantitatively in a simple phenomenological feedback model for light adaptation (Tranchina et al., 1984; Tranchina and Peskin, 1988).

Fig. 13 summarizes relationships in the model among sensitivity, cGMP flux (guanylate cyclase activity), $[Ca^{2+}]_i$, and [cGMP]. Fig. 13 *a* plots relative flash sensitivity (S_F/S_F^D vs. the steady cGMP flux established by each background light level for intensities spanning the range used in our experiment study. Fig. 13 *b* plots S_F/S_F^D vs. steady $[Ca^{2+}]_i$, and S_F/S_F^D vs. steady [cGMP] established by each background light level.

Deficiencies of the model

The step responses of the model with electrogenic Na^+/K^+ exchange are much like those of the previous simpler model, illustrated by Sneyd and Tranchina (1989, Fig. 6), and reach a plateau too quickly compared with the step responses of real cones. Discrepancies between the tails of theoretical and experimental step responses are reflected in the frequency domain as discrepancies in the temporal frequency responses at low frequencies. Comparison of the step responses of our model (cf. Fig. 6 of Sneyd and Tranchina, 1989) with those of real cones (see Fig. 18 of Baylor et al., 1974*a*; Fig. 6 of Normann and Perlman, 1979) indicates that our

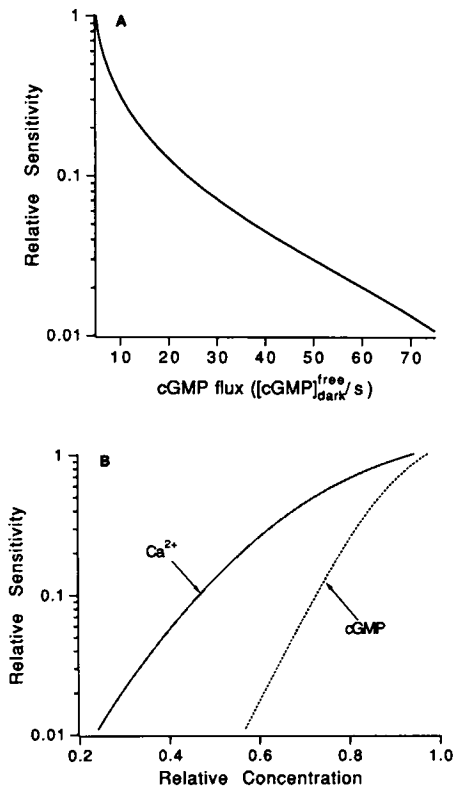

FIGURE 13 (*A*) Relationship between relative flash sensitivity (S_F/S_F^D) and steady cGMP flux, g, established at each background light level for I_0 in the range 5×10^{-5} to 5×10^{-1}. (*B*) Relationship between S_F/S_F^D and steady $[Ca^{2+}]_i$ (*solid curve*), and between S_F/S_F^D and steady [cGMP] (*dotted curve*) established at each background light level.

model lacks a process which acts on a time scale of several hundred ms to restore the membrane potential back toward the dark potential following a step of illumination. One possible candidate for the underlying mechanism, which seems to have the right time scale, is the time- and voltage-dependent conductance in the cone membrane characterized in detail by Barnes and Hille (1989) for salamander cones, and by Maricq and Korenbrot (1990) for lizard cones.

Copenhagen and Green (1987) and Itzhaki and Perlman (1987) demonstrated that adaptation can spread in the network of electrically coupled turtle cones (Detwiler and Hodgkin, 1979). That is, illumination of the retina by a narrow bar, for example, will cause a decrease in sensitivity in photoreceptors near the bar but receiving no illumination. The spread of adaptation has the same space scale as the spread of voltage in the network. Copenhagen and Green (1987) hypothesize that the spread of adaptation is mediated in part by a voltage-dependent conductance in the membrane of the cone inner segment, but Green and Glover (1989) showed that a voltage-dependent conductance alone cannot account for this phenomenon. Our model also cannot account for the apparently related finding of Lamb and Simon (1977): that injection of a hyperpolarizing current into cones causes a desensitization of the response to light, while a depolarizing current causes an increase in sensitivity. It is presently unclear whether Ca^{2+} or some other messenger for adaptation might be involved in these phenomena. It is conceivable that hyperpolarization of the cone, even in the absence of light, leads to a reduction in $[Ca^{2+}]_i$ because of the voltage dependence of the Na^+/Ca^{2+}-K^+ exchange pump (Lagando et al., 1988; Cervetto et al., 1989), and that this reduction gives adaptation. However, this mechanism would require a steeper voltage dependence of the exchange pump rate than the Ca^{2+} component of the light-sensitive current. In any case, our model, in which voltage dependence of conductances and pump rates is ignored, cannot account for the spread of adaptation or the effects of membrane polarization on sensitivity.

Implications of model parameters

The following conclusions are based on the interpretation of model parameters given in Table 2 and the parameter values in Table 3. In the model, the ratio of the maximal hydrolytic rate of phosphodiesterase (i.e., if 100% of PDE were suddenly activated to PDE*) to that in the dark is given by $(\gamma + \delta)/\delta$. With the assumption that $\delta = 5\ s^{-1}$, we found this ratio to be in the range of 46–115 with an average value of 62.

According to the model, the saturation of PDE* plays essentially no role in adaptation over the four lowest light levels used in our study. The light level at which half the phosphodiesterase is in activated form ($I_0 = \beta/\eta$) was in the range of 0.23–1.1 (relative units) with an average value of 0.7. Recall that the highest light level used was $I_0 = 0.5$.

The time constant for the decay of PDE* ($1/\beta$) was in the range of 14–60 ms with an average value of 30 ms.

The time constant for the decay of current from the Na^+/Ca^{2+}-K^+ exchange pump, when all the light-sensitive channels are closed, was in the range of 44–74 ms with an average value of 58 ms. Nakatani and Yau (1988) report that they found a time constant of roughly 0.1 s in their own cone experiments (Yau and Nakatani, 1988), and imply that Cobbs and Pugh (1986) found similar values in cones.

The membrane time constant, when all light-sensitive channels are closed, τ_m, was in the range of 14–19 ms with an average value of 17 ms.

The capacitance of the cone membrane, C, can be estimated from the value of τ_m as follows. In the model, the light-sensitive current in darkness, i_{dark}, is $-3EG/2$,

and $\tau_m = C/G$. Therefore, $C = -2i_{dark}\tau_m/(3E)$. If we assume that i_{dark} = 60 pA (Cobbs et al., 1985), then we find that C for the model cone was in the range of 39–63 pF with an average value of 49 pF. These numbers are about a factor of 2 lower than an estimate of 85 pF for the cone membrane capacitance in the tiger salamander (Attwell et al., 1982) and a previous estimate of 100 pF for turtle cones (Detwiler and Hodgkin, 1979). However, more recently, Barnes and Hille (1989) found that their mechanically isolated tiger salamander cones had an average capacitance of 31 pF.

Concluding remarks

It is important to note that there is recent evidence for an additional noncalcium-dependent mechanism for light adaptation in rods (Kawamura and Murakami, 1989). Experiments by Sather et al. (1988) and Rispoli and Detwiler (1989) also indicate an adaptive mechanism dependent on light as well as reduction in $[Ca^{2+}]_i$. Thus, modifications of our model may be necessary.

We note that the involvement of nonlinearities in cGMP and voltage kinetics, and phosphodiesterase saturation in light adaptation in the model, might possibly help to explain the findings of Nicol and Bownds (1989), which suggested that Ca^{2+} does not regulate all aspects of light adaptation in rods.

The speeding up of the decay of the flash response of the model with increasing background light, under conditions of fixed $[Ca^{2+}]_i$ is a feature that is intrinsic to the structure of the model: it arises from the fact that the hydrolysis of cGMP proceeds at a rate proportional to the product of [PDE*] and [cGMP]. The effective time constant for the change in [cGMP] when there is a small perturbation in PDE* from a steady state is $[\delta[1 + I_0(\gamma/\delta)(\eta/\beta)]]^{-1}$; this conclusion comes from the following analysis of the linearized system of equations.

We consider a stimulus of the form $I(t) = I_0 + \epsilon I_1(t)$, where ϵ is a small parameter. Then each of the dynamic variables can be expressed as a Taylor series in ϵ. If we keep only terms to first order in ϵ, then $s(t) = s_0 + \epsilon s_1(t)$; $p(t) = p_0 + \epsilon p_1(t)$; $x(t) = x_0 + \epsilon x_1(t)$; etc. Putting the expressions above for $p(t)$ and $x(t)$ into Eq. 7 and equating terms on the left and right that are first order in ϵ gives,

$$\frac{1}{\delta + \gamma p_0}\frac{dx_1}{dt} + x_1 = -\frac{\gamma x_0}{\delta + \gamma p_0}p_1 .$$

Therefore, the time constant for the change in [cGMP] elicited by a change in [PDE*] is $[\delta + \gamma p_0]^{-1}$. By evaluating the system of Eqs. 6, 10, and 11 in the steady state, we find that $p_0 = (\eta/\beta)I_0/[1 + (\eta/\beta)I_0]$. Over the four lowest light levels used in our study, $p_0 \approx (\eta/\beta)I_0$. Therefore, the cGMP time constant is approximately equal to $[\delta + \gamma(\eta/\beta)I_0]^{-1} = [\delta[1 + (\gamma/\delta)(\eta/\beta)I_0]]^{-1}$.

Thus, the extent to which response kinetics change when $[Ca^{2+}]_i$ is fixed depends on a combination of parameters: when $I_0(\gamma/\delta)(\eta/\beta)$ becomes comparable to 1, as I_0 increases, response kinetics will change. To see this experimentally, it must happen at low enough background light levels where cGMP is not largely depleted, i.e., where photocurrent is not near saturation. In our model, this situation does obtain. This suggests that a good test of our model would be to measure photocurrent responses to flashes superimposed on background lights under conditions of fixed $[Ca^{2+}]_i$.

It is not clear to what extent our model will be applicable to the primate. A recent frequency-domain analysis of light adaptation in the primate (Purpura et al., 1990) shows striking similarities between families of temporal frequency responses of monkey retinal ganglion cells, turtle horizontal cells, and cones (compare Fig. 1 of Purpura et al., 1990, Fig. 1 of Tranchina et al., 1984, and Fig. 3 of this paper). However, the data of Schnapf et al. (1990) suggest that Weber's law behavior in primate retinal ganglion cells is not mediated primarily by adaptive mechanisms in the cones. Furthermore, Schnapf et al. (1990) have presented evidence that light adaptation in primate cones differs in some respects from that in turtle cones. Although the dependence of flash sensitivity on background light follows the Weber-Fechner relation in primate cones, there is little change in response kinetics with background light. In addition, the inferred time constant for change in $[Ca^{2+}]_i$ in primate cones (Schnapf et al., 1990) is several times larger than that reported for cones of lower vertebrates (Cobbs and Pugh, 1986; Nakatani and Yau, 1988) and also larger than the value we infer here for turtle cones. The time course with which adaptation occurs in primate cones is consistent with the inferred time scale of Ca^{2+} kinetics (Schnapf et al., 1990). To develop a universal model for phototransduction, one would have to show that modifications of our model could account for the behavior of primate cones. These modifications might include a change in the guanylate cyclase activity function and a change in Ca^{2+} kinetics, e.g., by inclusion of a slower buffer and/or coupling between $[Ca^{2+}]_i$ and $[Na^+]_i$.

We thank Norman Milkman and Michelangelo Rossetto for design, construction, and programming of equipment used in this study. We also thank Charles Peskin for his help in many aspects of this work.

This work was supported National Eye Institute grants EY05991 and Core grant EY01842, National Science Foundation (NSF) grant BNS8919993, a Whitehead fellowship (Dr. Tranchina), The New York University Scientific Equipment Fund, and NSF grant DMS-8701895 (Dr. Sneyd). Dr. Sneyd was also supported in part by the University of California, Los Angeles.

Received for publication 12 December 1990 and in final form 27 March 1991.

REFERENCES

Attwell, D., F. S. Werblin, and M. Wilson. 1982. The properties of single cones isolated from the tiger salamander retina. *J. Physiol.* 328:259–283.

Barkdoll III, A. E., A. Sitaramayya, and E. N. Pugh Jr. 1986. Hydrolysis of 8-bromo-cGMP by light-sensitive phosphodiesterase of toad retinal rods. *Biophys. J.* 49:279*a*. (Abstr.)

Barkdoll III, A. E., E. N. Pugh, Jr., and A. Sitaramayya. 1989. Calcium dependence of the activation and inactivation kinetics of the light-activated phosphodiesterase of retinal rods. *J. Gen. Physiol.* 93:1091–1108.

Barnes, S., and B. Hille. 1989. Ionic channels of the inner segment of tiger salamander cone photoreceptors. *J. Gen. Physiol.* 94:719–743.

Baylor, D. A. 1987. Photoreceptor signals and vision. *Invest. Opthalmol. & Visual Sci.* 28:34–49.

Baylor, D. A., and A. L. Hodgkin. 1973. Detection and resolution of visual stimuli by turtle photoreceptors. *J. Physiol.* 234:163–198.

Baylor, D. A., and A. L. Hodgkin. 1974. Changes in time-scale and sensitivity in turtle photoreceptors. *J. Physiol.* 242:729–758.

Baylor, D. A., M. G. F. Fuortes, and P. M. O'Bryan. 1971. Receptive fields of cones in the retina of the turtle. *J. Physiol.* 214:265–294.

Baylor, D. A., A. L. Hodgkin, and T. D. Lamb. 1974*a*. The electrical response of turtle cones to flashes and steps of light. *J. Physiol.* 242:685–727.

Baylor, D. A., A. L. Hodgkin, and T. D. Lamb. 1974*b*. Reconstruction of the electrical responses of turtle cones to flashes and steps of light. *J. Physiol.* 242:759–791.

Baylor, D. A., B. J. Nunn, and J. L. Schnapf. 1984. The photocurrent, noise, and spectral sensitivity of rods of the monkey, *Macaca fascicularis*. *J. Physiol.* 357:575–607.

Burkhardt, D. A., J. Gottesman, and W. B. Thoreson. 1988. Prolonged depolarization in turtle cones evoked by current injection and stimulation of the receptive field surround. *J. Physiol.* 407:329–348.

Cervetto, L., L. Lagando, R. J. Perry, and D. W. Robinson. 1989. Extrusion of calcium from rod outer segments is driven by both sodium and potassium gradients. *Nature (Lond.)*. 337:740–743.

Chappell, R. L., K.-I. Naka, and M. Sakuranaga. 1985. Dynamics of turtle horizontal cell response. *J. Gen. Physiol.* 86:423–453.

Cobbs, W. H., and E. N. Pugh Jr. 1986. Two components of outer segment membrane current in salamander rods and cones. *Biophys. J.* 49:280*a*. (Abstr.)

Cobbs, W. H., A. E. Barkdoll III, and E. N. Pugh Jr. 1985. Cyclic GMP increases photocurrent and light sensitivity of retinal cones. *Nature (Lond.)*. 317:64–66.

Copenhagen, D. R., and D. G. Green. 1987. Spatial spread of adaptation within the cone network of the turtle retina. *J. Physiol.* 393:763–776.

Daly, S. J., and R. I. Normann. 1985. Temporal information processing in cones: effects of light adaptation on temporal summation and modulation. *Vision Res.* 25:1197–1206.

Dawis, S. M., R. M. Graeff, R. A. Heyman, T. F. Walseth, and N. D. Goldberg. 1988. Regulation of Cyclic GMP metabolism in toad photoreceptors. *J. Biol. Chem.* 263:8771–8785.

Detwiler, P. B., and A. L. Hodgkin. 1979. Electrical coupling between cones in the turtle retina. *J. Physiol.* 291:75–100.

Detwiler, P. B., and G. Rispoli. 1989. Phototransduction in detached rod outer segments: calcium control of the cGMP economy. *Investigative Ophthalmology and Visual Science.* 30(Suppl.):162.

Fain, G. L., and H. R. Matthews. 1990. Calcium and the mechanism of light adaptation in vertebrate photoreceptors. *Trends Neurosci.* 13:378–384.

Forti, S., A. Menini, G. Rispoli, and V. Torre. 1989. Kinetics of phototransduction in retinal rods of the newt *Triturus cristatus*. *J. Physiol.* 419:265–295.

Goldberg, N. D., A. Ames III, J. E. Gander, and T. F. Walseth. 1983. Magnitude of increases in retinal cGMP metabolic flux determined by ^{18}O incorporation into nucleotide α-phosphoryls corresponds with intensity of photic stimulation. *J. Biol. Chem.* 258:9213–9219.

Green, D. G., and M. J. Glover. 1989. Comparison of extrinsic current and background light desensitization of turtle cones. *Investigative Ophthalmology and Visual Science.* 30(Suppl.):65.

Haynes, L., and K.-W. Yau. 1985. Cyclic GMP-sensitive conductance in outer segment of catfish cones. *Nature (Lond).* 317:61–64.

Hodgkin, A. L., and B. J. Nunn. 1988. Control of light-sensitive current in salamander rods. *J. Physiol.* 403:439–471.

Hodgkin, A. L., P. A. McNaughton, and B. J. Nunn. 1987. Measurement of sodium-calcium exchange in salamander rods. *J. Physiol.* 391:347–370.

Itzhaki, A., and I. Perlman. 1987. Light adaptation of red cones and L1-horizontal cells in the turtle retina: effect of the background spatial pattern. *Vision Res.* 27:685–696.

Kawamura, S., and M. Murakami. 1986. In situ cGMP phosphodiesterase and photoreceptor potential in *Gecko* retina. *J. Gen. Physiol.* 87:737–759.

Kawamura, S., and M. Murakami. 1989. Regulation of cGMP levels by guanylate cyclase in truncated frog rod outer segments. *J. Gen. Physiol.* 94:649–668.

Koch, K.-W., and L. Stryer. 1988. Highly cooperative feedback control of retinal rod guanylate cyclase by calcium ions. *Nature (Lond.)*. 334:64–66.

Lagando, L., L. Cervetto, and P. A. McNaughton. 1988. Ion transport by the Na-Ca exchange in isolated rod outer segments. *Proc. Natl. Acad. Sci. USA.* 85:4548–4552.

Lamb, T. D. 1986. Transduction in vertebrate photoreceptors: the roles of cyclic GMP and calcium. *Trends Neurosci.* 9:224–228.

Lamb, T. D. 1987. Sources of noise in photoreceptor transduction. *J. Optical Society of America A.* 4:2295–2300.

Lamb, T. D., and E. J. Simon. 1977. Analysis of electrical noise in turtle cones. *J. Physiol.* 272:435–468.

Lamb, T. D., P. A. McNaughton, and K.-W. Yau. 1981. Spatial spread of activation and background desensitization in toad rod outer segments. *J. Physiol.* 319:463–496.

Liebman, P. A., K. R. Parker, and E. A. Dratz. 1987. The molecular mechanisms of visual excitation and its relation to the structure and composition of the rod outer segment. *Annu. Rev. Physiol.* 49:765–791.

Lolley, R. N., and E. Racz. 1982. Calcium modulation of cyclic GMP synthesis in rat visual cells. *Vision Res.* 22:1481–1486.

Maricq, A. V., and J. I. Korenbrot. 1990. Inward rectification in the inner segment of single cone photoreceptors. *J. Neurophysiol.* 64:1917–1928.

Matthews, H. R., R. L. W. Murphy, G. L. Fain, and T. D. Lamb. 1988. Photoreceptor light adaptation is mediated by cytoplasmic calcium concentration. *Nature (Lond.)*. 334:67–69.

Matthews, H. R., G. L. Fain, R. L. W. Murphy, and T. D. Lamb. 1990. Light adaptation in cone photoreceptors of the salamander: a role for cytoplasmic calcium. *J. Physiol.* 420:447–469.

Naka, K.-I., M.-O. Itoh, and R. L. Chappell. 1987. Dynamics of turtle cones. *J. Gen. Physiol.* 89:321–337.

Nakatani, K., and K.-W. Yau. 1988. Calcium and light adaptation in retinal rods and cones. *Nature (Lond.).* 334:69–71.

Nakatani, K., T. Tamura, and K.-W. Yau. 1990. Calcium feedback and sensitivity regulation in primate rods. *Society for Neuroscience Abstracts.* 16:part 1, 465.

Nicol, G. D., and M. D. Bownds. 1989. Calcium regulates some, but not all, aspects of light adaptation in rod photoreceptors. *J. Gen. Physiol.* 94:233–259.

Normann, R. A., and I. Perlman. 1979. The effects of background illumination on the photoresponses of red and green cones. *J. Physiol.* 286:491–507.

O'Bryan, P. M. 1973. Properties of the depolarizing synaptic potential evoked by peripheral illumination in cones of the turtle retina. *J. Physiol.* 235:207–223.

Pugh, E. N. Jr, and W. H. Cobbs. 1986. Visual transduction in vertebrate rods and cones: a tale of two transmitters, calcium and cyclic GMP. *Vision Res.* 26:1613–1643.

Pugh, E. N. Jr., and T. D. Lamb. 1990. Cyclic GMP and calcium: messengers of excitation and adaptation in vertebrate photoreceptors. *Vision Res.* 30:1923–1948.

Purpura, K., D. Tranchina, E. Kaplan, and R. M. Shapley. 1990. Light adaptation in the primate retina: analysis of changes in gain and dynamics of monkey retinal ganglion cells. *Visual Neuroscience.* 4:75–93.

Ratto, G. M., R. Payne, W. G. Owen, and R. Y. Tsien. 1988. The concentration of cytosolic free calcium in vertebrate rod outer segments measured with fura-2. *J. Neurosci.* 8:3240–3246.

Rispoli, G., and P. B. Detwiler. 1989. Light adaptation in Gecko rods may involve changes in both the initial and terminal stages of the transduction cascade. *Biophys. J.* 55:380*a*. (Abstr.)

Sather, W. A., G. Rispoli, and P. B. Detwiler. 1988. Effects of calcium on light adaptation in detached Gecko rod outer segments. *Biophys. J.* 53:390*a*. (Abstr.)

Schnapf, J. L., B. J. Nunn, M. Meister, and D. A. Baylor. 1990. Visual transduction in cones of the monkey *Macaca fasicularis. J. Physiol.* 427:681–713.

Shapley, R. M., and C. Enroth-Cugell. 1984. Visual adaptation and retinal gain controls. *In* Progress in Retinal Research. N. Osborne and G. Chader, editors. Pergamon Press, London. 263–346.

Sitaramayya, A., J. Harkness, J. Parks, C. Gonzales-Ovivia, and P. A. Liebman. 1986. Kinetic studies suggest that light-activated cyclic GMP phosphodiesterase is a complex with G-protein subunits. *Biochemistry.* 25:651–656.

Sneyd, J., and D. Tranchina. 1989. Phototransduction in cones: an inverse problem in enzyme kinetics. *Bull. Math. Bio.* 51:749–784.

Stieve, H., ed. 1986. The Molecular Mechanism of Photoreception. Springer-Verlag, New York.

Stryer, L., 1986. Cyclic GMP cascade of vision. *Annu. Rev. Neurosci.* 9:87–119.

Torre, V. 1982. The contribution of the electrogenic sodium-potassium pump to the electrical activity of toad rods. *J. Physiol.* 333:315–341.

Tranchina, D., and C. S. Peskin. 1988. Light adaptation in the turtle retina: embedding a parametric family of linear models in a single non-linear model. *Visual Neuroscience.* 1:339–348.

Tranchina, D., J. Gordon, and R. Shapley. 1984. Retinal light adaptation—evidence for a feedback mechanism. *Nature (Lond.).* 310:314–316.

Tranchina, D., J. Gordon, R. Shapley, and J.-I. Toyoda. 1981. Linear information processing in the retina: a study of horizontal cell responses. *Proc. Natl. Acad. Sci. USA.* 78:6540–6542.

Tranchina, D., J. Gordon, and R. Shapley. 1983. Spatial and temporal properties of luminosity horizontal cells in the turtle retina. *J. Gen. Physiol.* 82:573–598.

Wessling-Resnick, M., and G. L. Johnson. 1987. Allosteric behavior in transducin activation mediated by rhodopsin. *J. Biol. Chem.* 8:3697–3705.

Yau, K.-I., and D. A. Baylor. 1989. Cyclic GMP-activated conductance of retinal photoreceptor cells. *Annu. Rev. Neurosci.* 12:289–327.

Yau, K.-W., and K. Nakatani. 1984. Electrogenic Na-Ca exchange in retinal rod outer segment. *Nature (Lond.).* 311:661–663.

Yau, K.-W., and K. Nakatani. 1985. Light-induced reduction of cytoplasmic free calcium in retinal rod outer segment. *Nature (Lond).* 313:579–582.

Yau, K.-W., and K. Nakatani. 1988. Sodium-dependent efflux at the outer segment of the retinal cone. *Biophys. J.* 53:473*a*. (Abstr.)